



Research Paper

# RETROSPECTIVE CONSIDERATION OF A PLAUSIBLE VIBRATION MECHANISM FOR THE FAILURE OF THE FOLSOM DAM TAINTER GATE

Noriaki Ishii<sup>1\*</sup>, Keiko Anami<sup>2</sup> and Charles W Knisely<sup>3</sup>

\*Corresponding Author: Noriaki Ishii, ✉ [ishii@isc.osakac.ac.jp](mailto:ishii@isc.osakac.ac.jp)

A massive 87-ton Tainter gate installed at the Folsom Dam failed during operation on July 17, 1995. To avoid similar future failures all potential causes of the accident must be considered. For this purpose, experimental modal analyses were undertaken on one of the similarly designed remaining Tainter gates to identify its in-air natural vibration characteristics. The experimental mode shapes and frequencies are presented. Subsequently, a Finite-Element Method (FEM) model of the Folsom gate was constructed and validated by comparing the calculated natural vibration characteristics with the corresponding measured values. The validated FEM model was then used to calculate the static structural deformation of the Folsom gate and corresponding stresses. From the methodical investigation presented in this paper, the static loading due to increased trunnion friction on the Folsom Tainter gate was insufficient to produce failure. Finally, a conceptual model of a closed energy cycle for the self-excited vibration of the Folsom Dam Tainter gate is developed. This conceptual model was validated through tests on a two-dimensional 1/31-scale model of the failed Folsom gate.

Keywords: Folsom Dam gate, Tainter gate vibration, Radial gate, Failure investigation, Mode shape, Coupled-mode self-excited vibration

## INTRODUCTION

A radial gate (also called a “Tainter gate”) installed at the Folsom Dam in California, having a height of 15.5 m, a width of 12.8 m, a radius of 14.33 m and a mass of  $87.03 \times 10^3$

kg, failed early in the morning of July 17, 1995, as shown in Figure 1a, unleashing a thundering torrent of white-water. Figure 2a shows the view from downstream of the Folsom Dam Tainter gate before failure, while Figure 2b shows the

<sup>1</sup> Department of Mechanical Engineering, Osaka Electro-Communication University, 18-8, Hatsu-chou, Neyagawa, Osaka 572-8530, Japan.

<sup>2</sup> Department of Mechanical Engineering, Ashikaga Institute of Technology, 268 Omae-cho, Ashikaga, Tochigi 326-8558, Japan.

<sup>3</sup> Department of Mechanical Engineering, Bucknell University, Lewisburg, PA 17837, USA.

Figure 1: Two Tainter Gate Failures: (a) An 87-ton Gate at the Folsom Dam in the USA on July 17, 1995, and (b) A 37-ton Gate at the Wachi Dam in Japan on July 3, 1967 (Courtesy of the Asahi Newspaper Co. Ltd.)

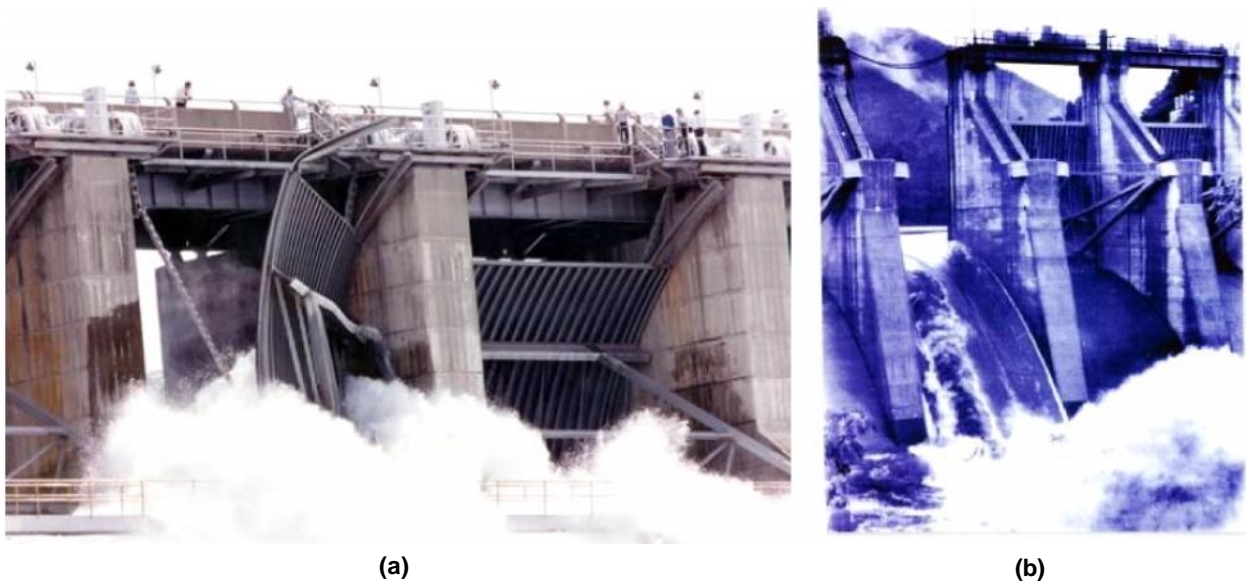


Figure 2: Two Views of Folsom Dam Tainter Gate: (a) Before Failure, and (b) After Failure



same gate after failure, opened like a hinged door and hanging on its massive chains.

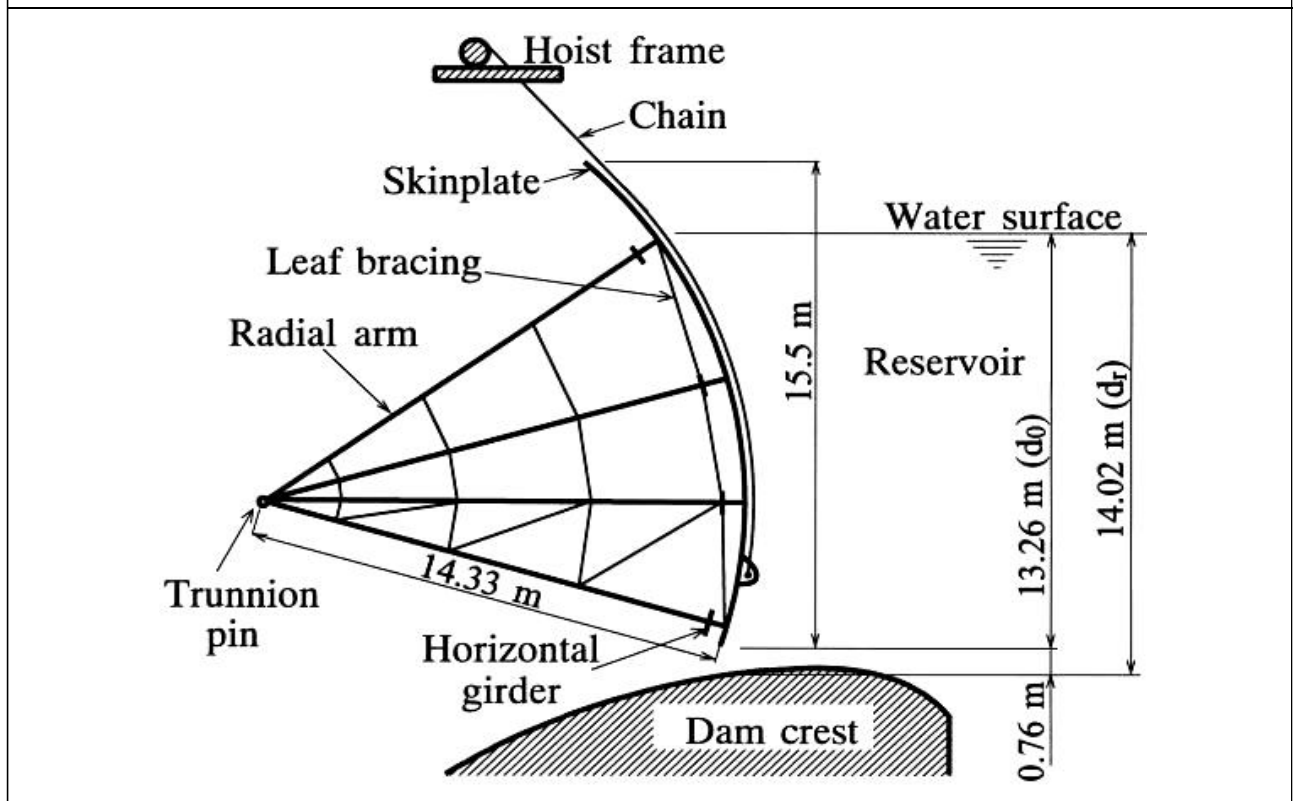
Figure 3 shows a side view of the Folsom Dam radial gate before failure. When the water depth over the dam crest was at 14.02 m, a routine gate opening operation was initiated. In an interview, the gate operator explained that when the gate opening reached 0.76 m, he was standing on the catwalk just above the gate. He felt a small steady vibration, which was initially very light, but intensifying very quickly. He pressed the stop button to stop raising the gate and, as he turned around, he saw the gate slowly emerging from the bay in the downstream direction like a large hinged garage door (Ishii, 1995a).

A different gate failure incident is portrayed in Figure 1b. A radial gate at the Wachi Dam

in Japan, with a height of 12 m, a width of 9 m, a radius of 13 m and a mass of 37 tons, failed and was swept about 140 m downstream on July 2, 1967 (Ishii and Imaichi, 1980). About 30 years ago, the review team for the gate failure in Japan suggested that flow-induced vibration was a possible cause of the failure. At that time, however, the detailed mechanism of such flow-induced vibration was unknown and the dynamic characteristics of radial gates were not well-studied.

In the investigation of the Tainter gate failure at the Wachi Dam, several studies were conducted by Ishii and Imaichi (1976, 1977a, 1977b and 1980) and Ishii and Naudascher (1984 and 1992), where it was assumed that the center of the circular-arc skinplate did not coincide, in general, with the trunnion center.

Figure 3: Side View Drawing of 87-ton Folsom Dam Tainter Gate

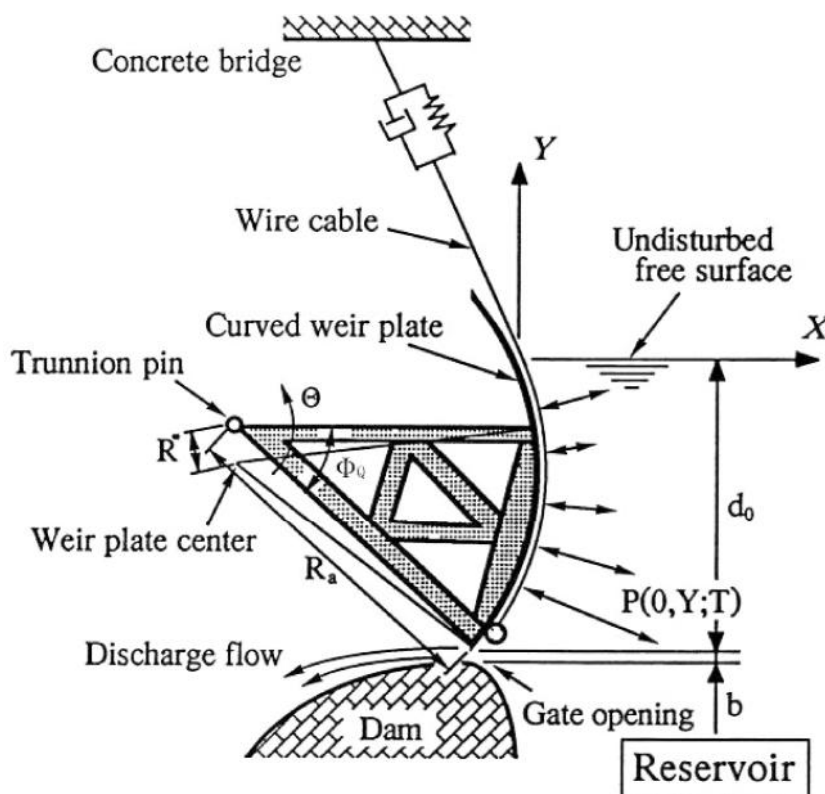


Such a Tainter gate is called an “eccentric Tainter gate”. When the skinplate center is shifted to a location beneath the trunnion pin, as shown in Figure 4, the fluid force acting on the skinplate tends to close the gate opening. A gate with such a design is called a “press-shut device”. The gate is statically stable, since the gate is pressed closed by the hydrostatic pressure. Such a gate, however, is not necessarily dynamically stable. In fact, in many cases, such a gate is dynamically unstable. When the skinplate moves downward, the approach flow is decelerated, thus increasing the fluid pressure. Supposing the skinplate center is below the trunnion pin, the increasing fluid force beneath the gate counters the hydrostatic load and raises the gate permitting

greater discharge. The increased discharge creates a low pressure region beneath the gate, adding to the hydrodynamic load and causing the gate to close. As this process is repeated, energy is supplied to the gate and the gate begins to undergo self-excited vibration. A stability criterion for this type of flow-induced vibration of Tainter gates has formulated by Ishii and Naudascher (1992).

The initial research after the Wachi failure focused on this “eccentricity instability” which requires a displacement of the skinplate center relative to the trunnion pin. Since the failed Wachi gate did not have any significant eccentricity, the consensus at the time was that the self-excited vibration mechanism identified by Ishii could not have actually occurred.

Figure 4: Side View Drawing of an Eccentric Tainter Gate Suspended by a Spring and Damper



More than 28 years after the Wachi gate failure, the 87-ton Tainter gate failed at the Folsom Dam. The report of the failure on July 19, 1995 in *The Japan Times* included the following passage:

A 90-ton gate at Folsom Dam buckled Monday (July 17), unleashing a thundering white-water torrent ... The problem started as operators were reopening the huge metal gate—one of eight spillways—after the flow had been temporarily shut down. “We were opening the gate, and it started to vibrate. We don’t know why”, said Tom Aiken, dam manager for the US Bureau of Reclamation.

In this report, the dam manager for the USBR clearly indicates that vibrations played a role in the Folsom Dam gate failure. He had also previously mentioned the role of vibrations in the following excerpt from a televised press conference on July 17, 1995 (KXTV-10, 1995):

This morning at 8 o'clock we were making a routine gate change on our No. 3 spillway gate and our operator said he noticed something bind up a little bit and the gate vibrated and suddenly gave way and right now we have about 40,000 cubic ft/s being released.

On August 15, 1995, about a month after the gate failure, the first author had the opportunity to interview James Taylor, gate operator of the failed gate, who was standing on the catwalk just over the gate at the time of failure. He too indicated that vibrations accompanied the gate failure as follows:

When spill gate No. 3 reached around 2½ feet, I felt an unusual vibration. I

immediately pushed the stop button and started to check the gate. The vibration intensified and as I turned to check the gate, I could see the right side (looking downstream) of the gate separating from the structure and water coming out around the gate ...

Based on these clear eyewitness testimonies, some sort of vibration was evidently involved in the Folsom Dam Tainter gate failure. The Forensic Report concerning this failure assigns blame, however, to excessive static loading (due to increased trunnion friction) of cross braces with insufficient stiffness and strength. This conclusion is based on several runs of a finite element code that was not validated, but which produced results in agreement with the mode of failure—the failure of the bolts that connected Brace 3E-4D. The fact that this conclusion was at odds with eyewitness reports was essentially ignored.

Ishii (1995a) had an initial suspicion that “eccentricity instability” may have played a role in the Folsom Dam failure. The radial gate at the Folsom Dam, however, did not possess such an eccentricity between the skinplate center and trunnion center. The observations of the gate operator and, subsequently, the validated FEM model results (to be discussed subsequently in this paper) that were inconsistent with a static failure, lead naturally to consideration of a new mechanism for a “non-eccentricity hydrodynamic instability” to which non-eccentric radial gates may be susceptible. This new dynamic instability is a two degrees-of-freedom coupled-mode vibration resulting from the coupling of two vibration modes

through inertia forces and hydrodynamic forces acting on the gate.

As a first step in the exploration of a potential vibration mechanism for the Folsom Dam gate, in late September 1995, Ishii (1995b) conducted in-air experimental modal analysis on one of the remaining geometrically similar Folsom Dam gates (subsequently designated as the "original gate"), employing an impact hammer and accelerometers. From this modal analysis, a relatively precise assessment of the natural vibration characteristics of the failed gate was obtained. After this initial modal analysis, the remaining gates were reinforced. Subsequently, in the middle of November 1996, a similar experimental modal analysis was conducted on one of the reinforced Folsom Dam gates in order to evaluate the dynamic effectiveness of the reinforcement (Ishii, 1997).

The Finite-Element Method (FEM) has been developed over several decades and is now routinely used as a tool to identify natural frequencies and mode shapes. However, the method cannot provide information on damping ratios. Further, any FEM analysis contains many uncertainties, such as mass, stiffness and constraint conditions, which may significantly affect the results. Experimental modal analysis, on the other hand, can reliably identify the natural vibration mode shapes and frequencies, as well as the damping ratios. The drawback to experimental modal analysis of such large structures is the difficult, dangerous, and time intensive placement of expensive accelerometers. However, without such experimental input, the basic inherent uncertainties of the FEM analyses cannot be quantitatively assessed.

An FEM analysis was conducted on the original Folsom Dam gate, using a high precision finite element model with a large number of plate elements. The resulting calculated frequencies and mode shapes are presented and compared with the corresponding experimental results. The agreement between numerical and experimental mode shapes and frequencies allows the FEM uncertainties to be quantified. When the agreement is good, the FEM model has been validated. In addition, the static deformations and the static tensile loads were calculated for a range of frictional forces at the trunnion pins. These FEM deformations and loads contradict and call into question the conclusions of the USBR Forensic Report on the failed Folsom Dam Tainter gate. The claim that the gate failed due to excessive static loading brought about by increased trunnion friction and insufficient stiffness and strength in critical structural members could not be substantiated using the validated FEM model. The conclusions of the Forensic Report are also at odds with eyewitness accounts of vibration occurring just before failure.

In this study, the framework of the mechanism behind a dynamic instability of Tainter gates, unrelated to eccentricity of the gate, is presented. Its potential applicability to the failed Folsom Dam gate is detailed. Two inherent modes of structural vibration of the original Folsom Dam gate, as identified by in-air experimental modal analysis, are documented. In addition, similar in-air modal information is also presented for the reinforced Folsom gates. Impact force inputs, acceleration responses, and transfer functions are shown and used to identify the in-air natural

frequencies, mode shapes and the damping ratios.

The proposed dynamic instability mechanism, unrelated to gate eccentricity, involves the coupling of the rigid-body gate rotational vibration around the trunnion pins with a bending mode of the skinplate. The mechanism is formulated and presented in terms of a closed energy feedback cycle.

Finally, the existence of this proposed dynamic instability mechanism is demonstrated using a two-dimensional 1/31-scale model of the Folsom gate, where the lower-mode bending vibration of the skinplate is represented by a streamwise rotational vibration of the rigid model skinplate. The in-water natural frequency of the streamwise rotational skinplate vibration is fixed at two representative values, while the natural frequency of the whole gate vibration around the trunnion pin is varied over a wide range of values bracketing the in-water natural vibration frequency of the skinplate. The model gate was placed in a channel and exposed to flowing water. The gate vibration amplitudes were recorded.

## MATERIALS AND METHODS

The materials presented in this report have been drawn from three distinct, but related studies. The materials and methods for each of the individual studies are presented separately in the following sections.

### Experimental Modal Analysis of the Folsom Dam Tainter Gate

In late September 1995, an in-air experimental modal analysis was conducted on Tainter gate No. 2, a gate that is geometrically similar to

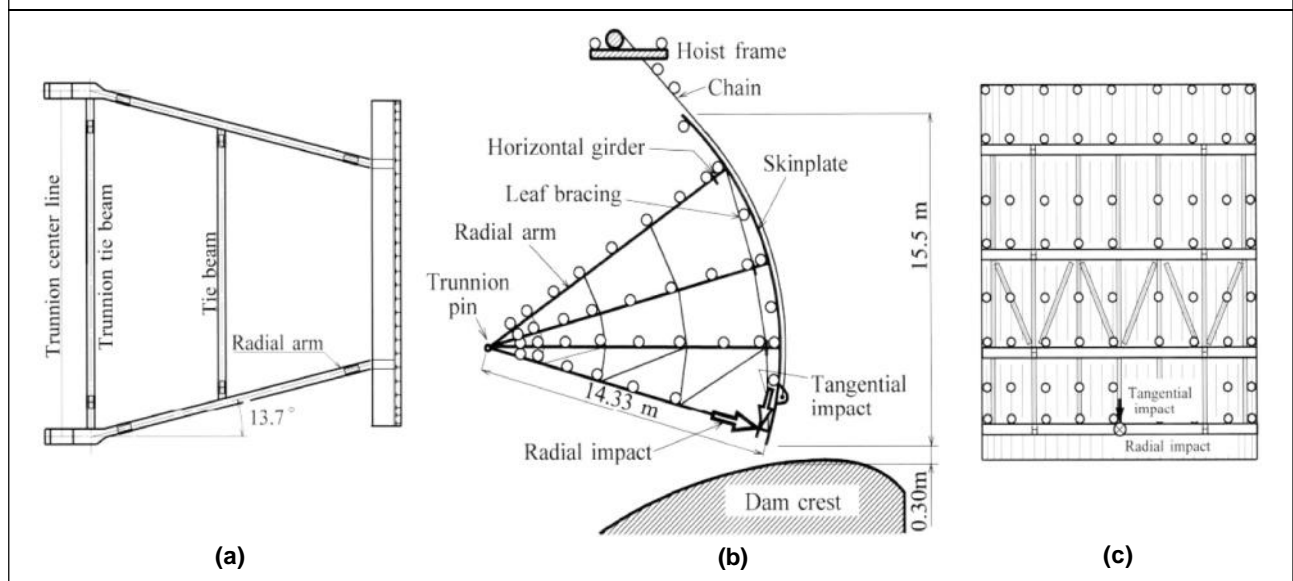
the failed Tainter gate. Subsequently, in mid-November 1996, a similar vibration test was undertaken on a reinforced Tainter gate.

As shown in Figure 3, the arm structure of the original gate had only two diagonal members between the lower two arms. The whole gate was hoisted by two chains with a length of 16.4 m, hooked to the gate near the bottom of the skinplate. A list of the mass of major members of the Folsom Dam Tainter gate is presented in Table 1, showing the mass of the skinplate with horizontal girders and leaf bracing was 59,732 kg, or about 68% of the whole gate mass of 87,033 kg.

To excite structural vibration of the gate, it was raised (with no water behind the gate) by about 0.3 m and struck with a 5.4 kg impact hammer (PCB GK-086B50) which was instrumented with a force transducer (PCB GK-206M06). The center of the lower horizontal girder was struck in both the radial and tangential directions, respectively, as shown by the arrows in Figure 5. The impact position was chosen to excite as effectively as possible structural vibration modes

Member	Mass (kg)
Skinplate & chain guide	24,786
Curved T-beam	16,264
Horizontal girders	16,283
Leaf bracings	2,399
Radial arm struts	15,561
Arm bracings	1,830
Tie beam	1,691
Trunnion pin	8,174
Others	45
<b>Total</b>	<b>87,033</b>

Figure 5: Radial and Tangential Impact Position ( $\otimes$ ) and Measurement Points ( $\circ$ ) for Experimental Modal Analysis of Folsom Dam Tainter Gate, Showing (a) Top View of the Gate, (b) Side View of the Gate, and (c) Upstream View of the Skinplate



associated with the bending flexibility of the skinplate and the radial arms. The radial impact was delivered by striking the flange center of the horizontal girder in the upstream direction, along the web line. The tangential impact was delivered by striking the web near the skinplate of the horizontal girder in the downward direction, perpendicular to the web.

The measurement locations of the gate acceleration responses to the impact force are identified by small circles in Figure 5. The acceleration responses were measured with accelerometers (GK-308B piezo-type by PCB Co. for the original gate, and LS-20C servo-type by RION Co. for the reinforced gate). In these tests 12 accelerometers, mounted on magnetic bases and positioned at various measurement locations, were used for each impact. For the skinplate vibrations, the accelerometers were systematically placed at 72 positions along the centers of the vertical beam flanges. For the radial arm vibrations,

the accelerometers were systematically placed at 64 positions along the center of the radial arm webs. In addition, the acceleration responses of the chains were measured at 2 positions on each chain to examine their lateral vibrations coupled with gate vibrations. The acceleration responses of the hoist frames supporting the reduction gear for chain winding were also measured to examine the effect of the chain elasticity on the gate vibrations. The hoist frame acceleration responses were recorded in the streamwise, vertical, and spanwise directions at 2 positions on each hoist frame. Additionally, the accelerometers were systematically placed at 18 positions on the cross beam webs to measure the radial and tangential acceleration responses. In total, acceleration responses were measured at 162 points.

On the skinplate, the radial (streamwise) and tangential acceleration responses were measured at each measurement location,



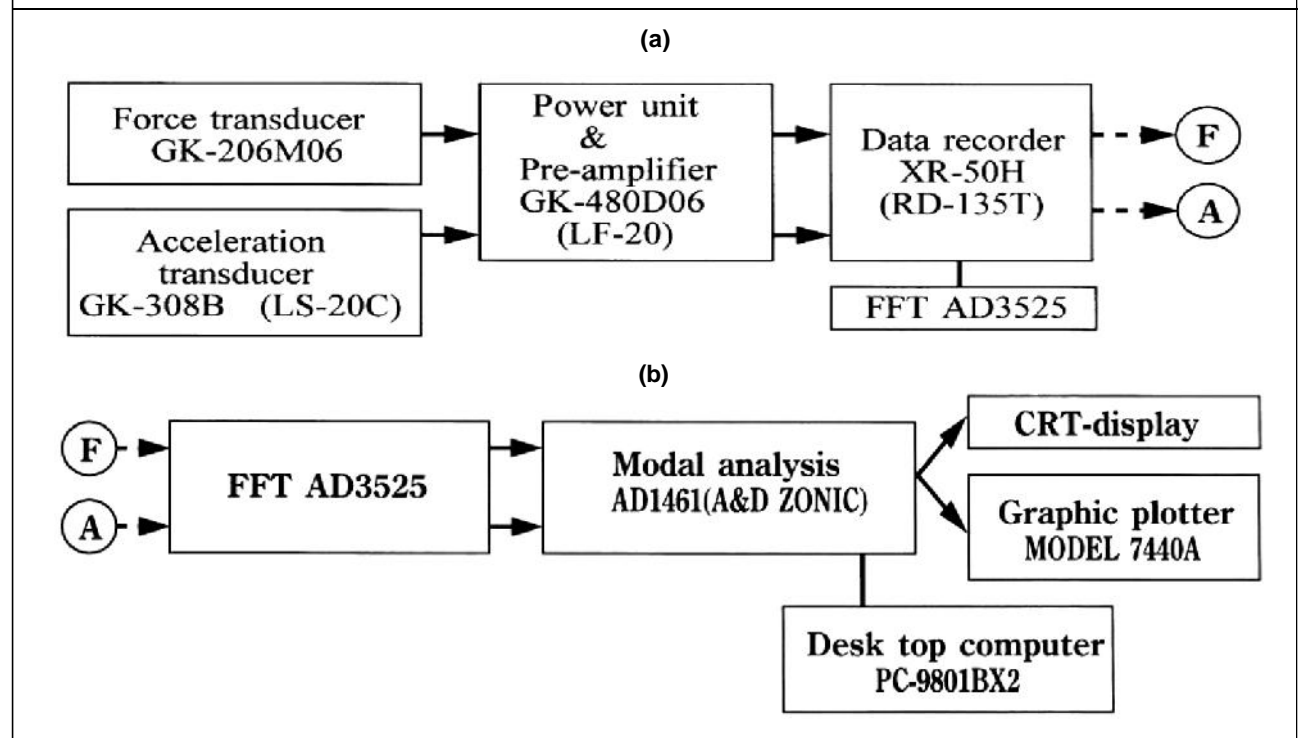
since vibration in the spanwise direction is insignificant. For measurement locations on the radial arms, however, vibrations in the tangential and spanwise directions were measured, since the vibration in the streamwise direction was less significant.

A schematic diagram of the instrumentation is shown in Figure 6a and the subsequent flowchart for the computer-based modal analysis is shown in Figure 6b. The circled “F” represents the impulsive force data, and the circled “A” the acceleration response data. The impact force data and the acceleration response data were amplified through dedicated exclusive amplifiers, and then recorded on tapes using a data recorder (XR-50H with VHS video tapes by TEAC Co. for the original gate, and RD-135T by TEAC Co. with digital audio tapes for the reinforced gate).

The recorded data were monitored using FFT analyzers (AD3525 by A&D Co.) to permit careful adjustment of the input levels to the data recorder for optimum recording.

**Precision FEM Model Development**  
 Based on the blueprint of the original Folsom Dam Tainter gate, a finite element model (frame structure) of the gate was created. Generally, in the Finite Element Method (FEM), simplified modeling is made in many cases. However, past experience suggests that for a complicated structure like a Tainter gate, the precision of the modeling has a significant influence on the accuracy of the subsequent output. For this reason, the model form was created faithfully in precise detail according to the blueprint, as discussed in Anami (2002) and Anami *et al.* (2006).

Figure 6: (a) Instrumentation, and (b) Data Processing Flowchart for Modal Analysis of the Folsom Dam Gate



The material properties of iron for all of the structures of Folsom gate were given as follows: 208.7 GPa for Young's modulus, 78.89 GPa for modulus of transverse elasticity, and 7,870 kg/m<sup>3</sup> for density. Correspondingly, Poisson's ratio was taken as 0.323.

The FEM gate model was created using standard elements: the "plate element", the "beam element" and the "DOF spring element". The plate element is a 2-dimensional element, consisting of 3 or 4 nodes, which has the advantage that the constraint conditions are given correctly, although the number of nodes increases. Thus, in addition to the skinplate itself, the main horizontal girders of the I-beam were also defined with 3 plate elements for the flanges and web. Furthermore, the H-beams of the radial arm and cross beam were also defined as 3 plate elements. The L-angle steel struts between the radial arms were defined by 2 plate elements.

The beam element can more simply model the structure as 2 nodes, but it is unsuitable for representing complicated constraint conditions. Therefore, in the present modeling, only the T-beams reinforcing the skinplate and the leaf-bracing L-angles were defined using the beam element, where each cross-sectional form was specified. The massive chains, which are attached to each spanwise side of the skinplate to hoist the gate, were defined as 1-DOF spring elements. The spring constant was  $0.718 \times 10^8$  N/m per chain, as calculated from the actual chain geometry.

In FEM analysis, the element division is a very significant aspect in determining the accuracy of the analysis results. It is trivial that the greater the element division number is, the more accurate are the results. However, the

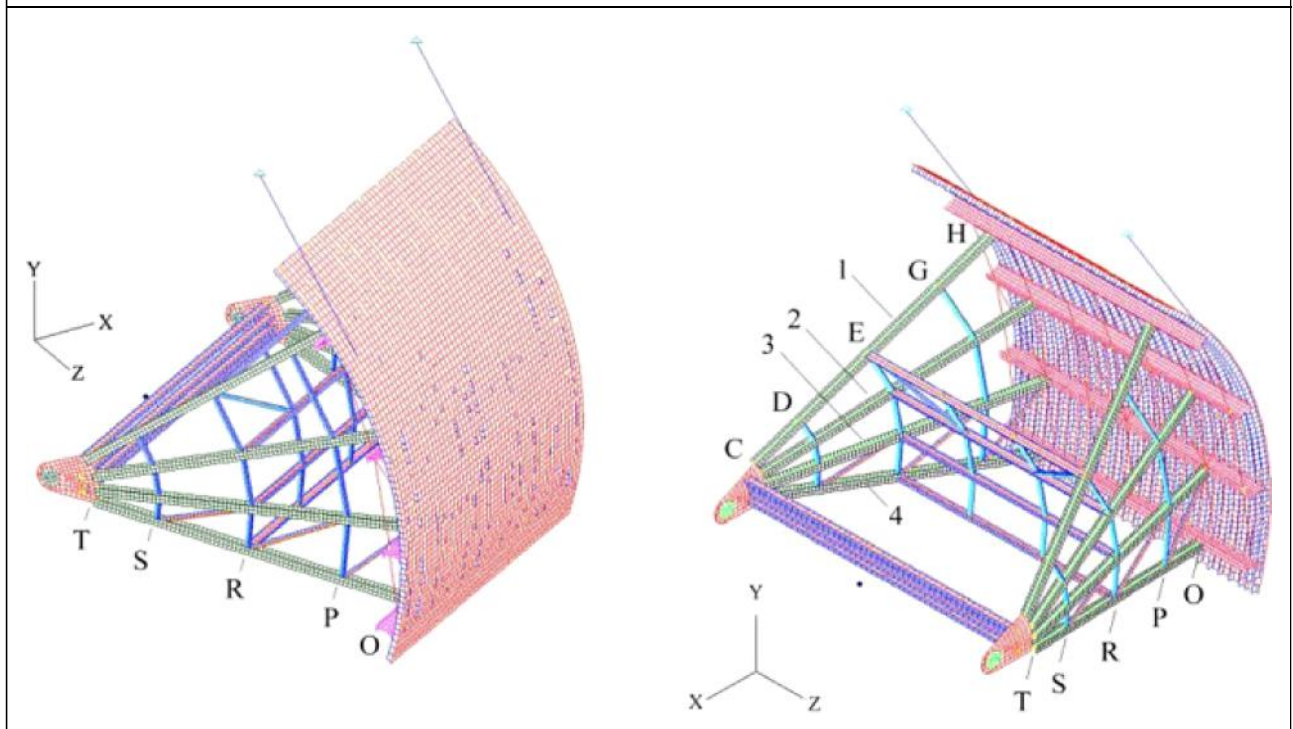
number of elements is restricted by the performance of the computer. Thus, it is necessary to make an effective analysis with the limited number of elements, where the element division was concentrated in the significant portions in the model. In the present analysis, the fine element divisions were made for the skinplate and radial arms, since the experimental modal analysis showed that they were significant factors in determining the natural vibrations of the whole gate. The total element number of the whole gate is 23,124, and the total nodes number is 23,967.

All structural elements were joined with bolts. Assuming sufficient rigidity, the junctions were specified as rigid constraint conditions. In this manner, high rigidity was given between one independent node and two or more subordinate nodes, thus enabling the transmission of the translation force and moment produced in the independent node to the subordinate nodes.

The trunnion pin is embedded in a concrete base, thus having only one degree of freedom to move around its rotation axis. Therefore, the flexibilities except for around its rotation axis were constrained for the trunnion pin. The chain ends have degrees of freedom in the rotational and translational directions, while the degree of freedom in the spanwise direction was constrained.

The high accuracy FEM model is shown in Figure 7, where the 3-dimensional views from the downstream and upstream sides are shown in Figures 7a and 7b, respectively. The points of intersection in these views are the element nodes. The elements surrounded by the nodes on the skinplate or on the radial arms are plate elements, and the lines connecting

Figure 7: Precise FEM Model Construction of the Original Folsom Dam Tainter Gate



the nodes of horizontal girders and skinplate reinforcement T-beams are beam elements. The numbers from 1 to 4 indicate the radial arms from the top. In order to identify the analysis results, the junctions of the arms and the trunnion pin hub on the right hand side are denoted "C", junctions of the arm struts and the vertical struts are denoted "D", "E" and "G" from the trunnion pin side, and junctions of the arm struts and the horizontal girders are denoted "H". The left hand junctions also are similarly denoted "T", "S", "R", "P" and "O" as shown in Figure 7.

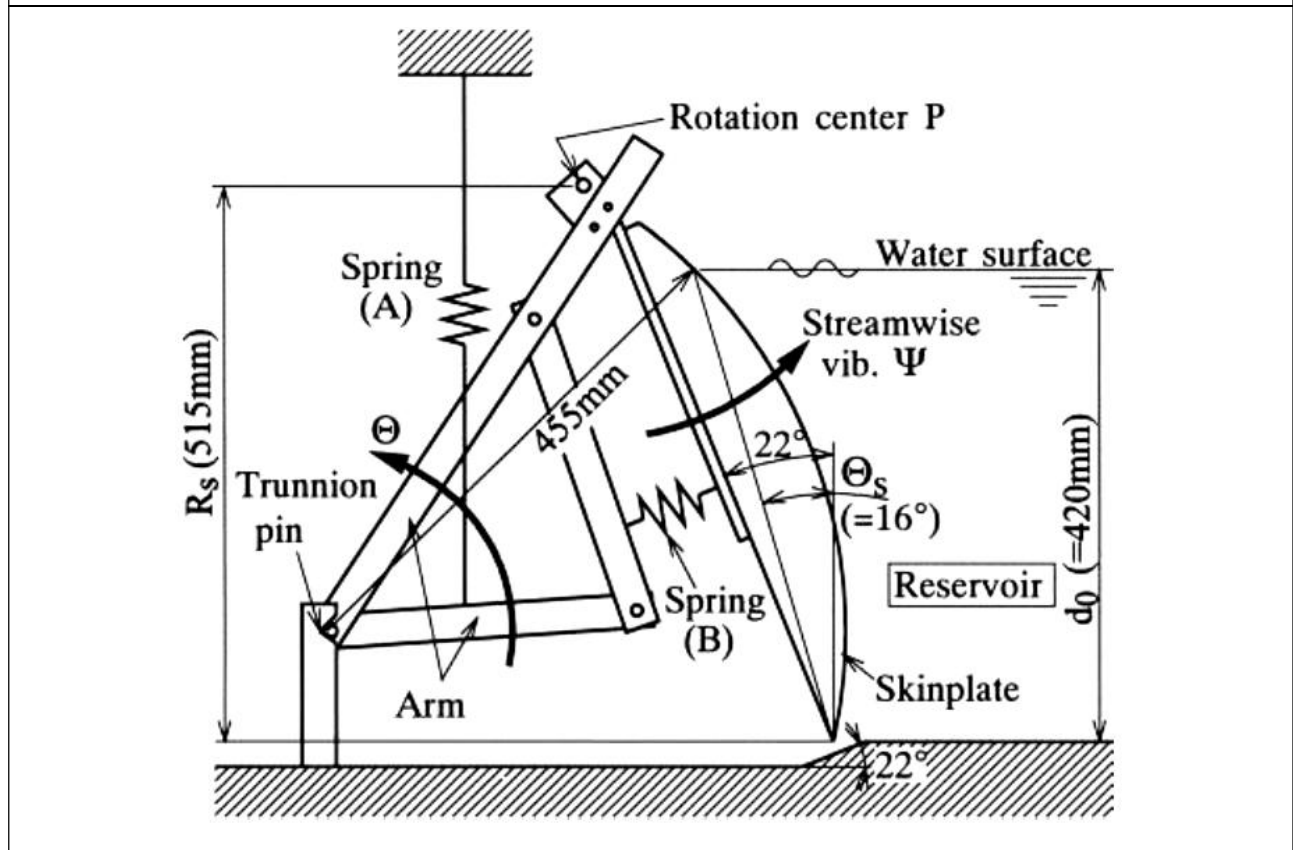
#### Design of 1/31-Scale Model

The major purpose of model gate testing was to obtain data concerning the coupled vibration of the streamwise skinplate bending rotation and the whole gate rotation, in order to confirm the coupled-mode self-excited vibration mechanism postulated later in this paper. The

data can also be used subsequently to verify the theoretical analysis of this mechanism. Once the theoretical analysis is verified, it can then be applied to calculate the hydrodynamic stability of the Folsom Dam gates, as well as of other gates, under various conditions. Fundamentally, the model gate does not necessarily need to be an exact scaled duplicate of Folsom Dam gate. Any combination of skinplate streamwise flexibility, skinplate rotation center height, and the in-air damping ratios and so on, are all possible for the model gate. Based on these model scale experiments, as well as on additional full-scale gate testing, Anami (2002) has developed a theoretical analysis that will be presented in a subsequent paper (Anami *et al.*, 2014).

The two-dimensional 1/31-scaled model gate is shown in Figure 8. The rigid skinplate is supported by a horizontal coiled spring (B)

Figure 8: Cross-Sectional View of a 1/31-Scaled Coupled-Mode Vibration Model of the Folsom Dam Gate



just behind the skinplate, which represents the streamwise skinplate bending elasticity in the full-scale gate. The skinplate has its rotation center placed on the radial arm for easy adjustment, and performs streamwise rotational vibrations, denoted by  $\Psi$ . The validity of such crude modeling was confirmed by the experimental modal analysis. The whole gate is suspended by a vertical coiled spring (A), which represents the chain elasticity in the full-scale gate. Thus, the gate performs rotational rigid-body vibrations around the trunnion pin, denoted by  $\Theta$ . The position of both the horizontal and vertical springs can be adjusted, thus permitting a fine adjustment of each natural vibration frequency. The model gate was so adjusted at static equilibrium with all

upstream heads that the skinplate center coincides exactly with the trunnion center, that is, it is non-eccentric. The streamwise vibration of the skinplate naturally shifts its center from the trunnion. However, assuming small-amplitude vibrations in this study, the eccentricity has a negligible effect in exciting the whole gate around the trunnion, when compared with that due to inertial torque of the skinplate itself.

The major specifications for the model gate are listed in Table 2. The skinplate has a radius  $R_s$  of 455 mm and a mass of 10.0 kg. The skinplate has a spanwise length  $W_0$  of 290 mm, and inserted in a 300 mm-wide channel, leaving a gap of about 5 mm from the channel

B	5 mm	$\Theta_{s0}$	0°	$W_0$	290 mm
$d_0$	420 mm	$\Theta_s$	16°	$R_c$	375 mm
$R_a$	455 mm	$\zeta_{a\theta}$	0.003	$R_s$	515 mm
$I_\theta$	2.220 kgm <sup>2</sup>	$\zeta_{a\psi}$	0.105	$\Omega_{a\psi}$	10.6 Hz
$I_\psi$	0.944 kgm <sup>2</sup>		0.133		12.3 Hz
$I_{\psi\theta}$	0.289 kgm <sup>2</sup>				

wall on each side of the skinplate. The whole gate has a mass of 15.1 kg. The skinplate rotation center height  $R_s$  from the skinplate lower end, shown in Figure 8 is 515 mm. The moment of inertia of the skinplate around its streamwise rotation center,  $I_\psi$ , takes a value of 0.944 kgm<sup>2</sup>, and the moment of inertia of the whole gate around trunnion pin,  $I_\theta$ , takes on a value of 2.220 kgm<sup>2</sup>.

It was significant in the model tests to adjust the in-water streamwise vibration frequency of the skinplate to be near that of the Folsom Dam Tainter gate, because the instantaneous coefficient of flow-rate-variation under the gate is strongly dependent upon the streamwise vibration frequency of the skinplate. From the field vibration tests, the in-air streamwise skinplate vibration frequency was found to be about 27 Hz. This in-air frequency is reduced in flowing water, due to the added mass effect of water upon the skinplate. With a calculated added mass, the in-water vibration frequency was estimated to be about 6 Hz (Anami and Ishii, 1998). In order to realize this in-water frequency in the present model tests, the in-air streamwise vibration frequency of the model skinplate,  $h_{rFE}$ , was set at one of two values, 10.6 Hz or 12.3 Hz

As shown in Figure 8, the skinplate is inclined downstream at an angle of 22°, similar

to the inclination of the Folsom Dam Tainter gate. The major purpose of the present model gate testing is to demonstrate the self-excited vibration due to the coupling of two inherent modes of vibration. For this reason, the channel floor just under the gate is inclined such that the press-open angle  $\Theta_{s0}$  becomes zero, thus eliminating the press-open hydrodynamic pressure component. With such a simplification of the model test setup, an easy physical understanding of the test results can be obtained.

The model gate was exposed to a water flow under the gate with an upstream submergence depth  $d_0$  of 420 mm. The outflow is not submerged. With given values of the gate submergence depth  $d_0$  and the skinplate in-air streamwise vibration frequency,  $h_{rFE}$ , the basic Froude number  $F_0$  which determines the dynamic similarity of fluctuating flow field, defined by

$$F_0 \equiv 2f \sqrt{\frac{d_0}{g}} \Omega_{a\psi} \dots(1)$$

takes on values of 13.9 and 16.0 in the present model tests. The gate opening mean height was adjusted to 5 mm, which is 1.2% of the gate submergence depth  $d_0$ . In the present model gate tests, the in-air whole gate vibration frequency  $\Omega_{r\psi}$  was varied from 2.6 Hz to 7.3 Hz, so as to include the in-water natural streamwise vibration frequency of the skinplate at around 6 Hz.

## RESULTS AND DISCUSSION

As in the section on the Materials and Methods, the results of each of the three studies will be reported sequentially, each successive one building on the results from the previous study.

Experimental Modal Analysis

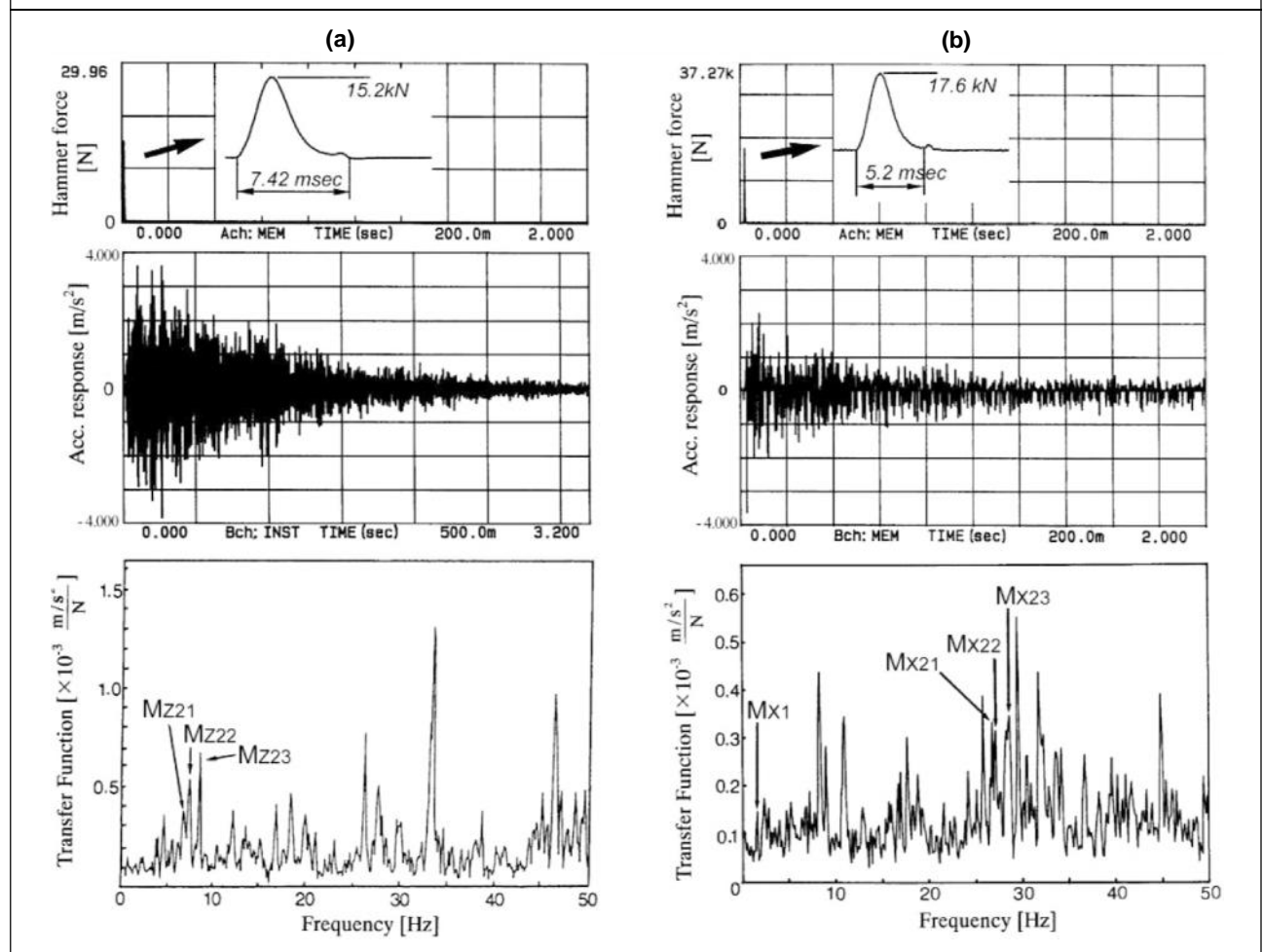
Calculation of Inverse Modal Indicator Functions (IMIF)

The recorded impulsive force and the acceleration response data were processed by the FFT analyzer (AD3525) to display the corresponding real time waveforms and to calculate their power spectra. As an example, the real time waves for the impulsive forces and the accelerations measured at the center of the skinplate are shown in Figure 9, where Figure 9a is for the tangential direction and Figure 9b for the radial direction. Typically, the

impulsive forces during about 5 to 8 ms reached a maximum level of about 15 to 17 kN. Each acceleration power spectrum was divided by the respective input impulsive force power spectrum to calculate the transfer functions. The impact tests were repeated three times for each acceleration response measurement location to permit averaging of the calculated transfer functions. The bottom plots in Figure 9 show the averaged transfer functions.

The calculated transfer functions at all 162 measurement locations were input into a

Figure 9: Representative Impulsive Input, Acceleration Response and Averaged Transfer Functions of In-Air Vibration of Folsom Dam Tainter Gate in (a) The Tangential (Up and Down) Direction, and (b) The Radial (Streamwise) Direction



software package for modal analysis (AD1461 by A&D ZONIC Co.) to calculate the Inverse Modal Indicator Functions (IMIF) as an average of all transfer functions, which is defined by

$$IMIF \equiv 1.0 - \frac{\sum_{i=1}^n [Real(T_i) \times |T_i|]}{\sum_{i=1}^n |T_i|^2} \quad \dots(2)$$

where  $T_i$  represents the  $i$ -th transfer function,  $Real(T_i)$  represents the real part of  $i$ -th transfer function, and  $|T_i|$  represents the amplitude of the transfer function. Therefore, the second term on right-hand side of Equation (2) represents  $\cos\{\}$  in which  $\{\}$  is the phase-lag of the vibration relative to the impulsive force, taking on a value of  $90^\circ$  in the resonance state. Thus, the peak level of IMIF represents the strength of the natural vibration of the gate. The calculated IMIF results are shown in Figure 10, where Figure 10a is for the tangential direction and Figure 10b is for the radial direction. All the peaks in the IMIF do not necessarily provide a reasonable mode shape. Detailed

examination of the vibration mode shapes was undertaken for each IMIF peak, permitting the identification of several meaningful mode shapes which exhibited orderly regularity in their amplitudes. The meaningful modes are identified by mode names on their corresponding IMIF peak in Figure 10. A subscript “z” in the mode names denotes a tangential (up-and-down, i.e., around the trunnion pin) mode shape, while a subscript “x” denotes a radial (streamwise direction) mode. The mode designations for these natural vibrations are also included on the transfer function plots in Figure 9.

Vibration Mode, Vibration Frequency and Damping Ratio

Major vibration modes are shown in Figure 11 and Figure 12, where Figures 11a and 12a show side views and Figures 11b and 12b show the 3D view of the gate. Figures 11c and 12c show the spanwise vibration amplitude distribution at labeled heights. The gray and black lines show the instantaneous vibration shapes with maximum amplitude. The

Figure 10: Inverse Modal Indicator Functions for In-Air Vibration of Folsom Dam Tainter Gate in (a) The Tangential (Up and Down) Direction, and (b) The Radial (Streamwise) Direction

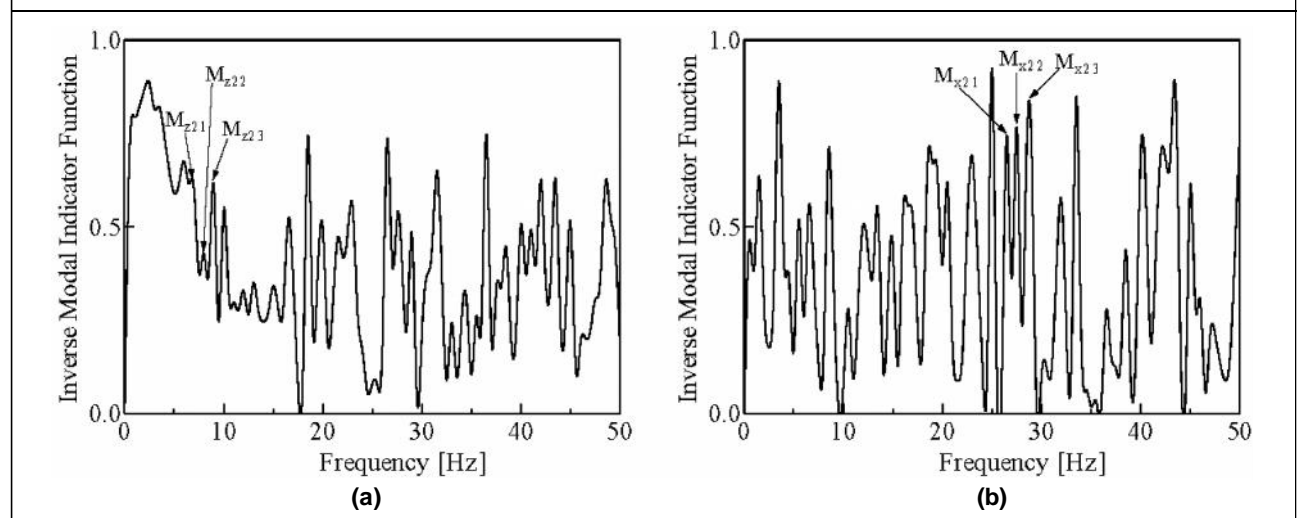


Figure 11: Fundamental Mode Shape of the Rigid Body (Whole Gate) Vibration Around the Trunnion Pin for the Original Folsom Dam Tainter Gate Designated as Mode  $M_{z2}$  ( $h_a = 6.88$  Hz;  $\zeta_a = 0.012$ ) Showing (a) The Side View, (b) A 3D-View, and (c) The Spanwise Distributions of Deflection Amplitudes

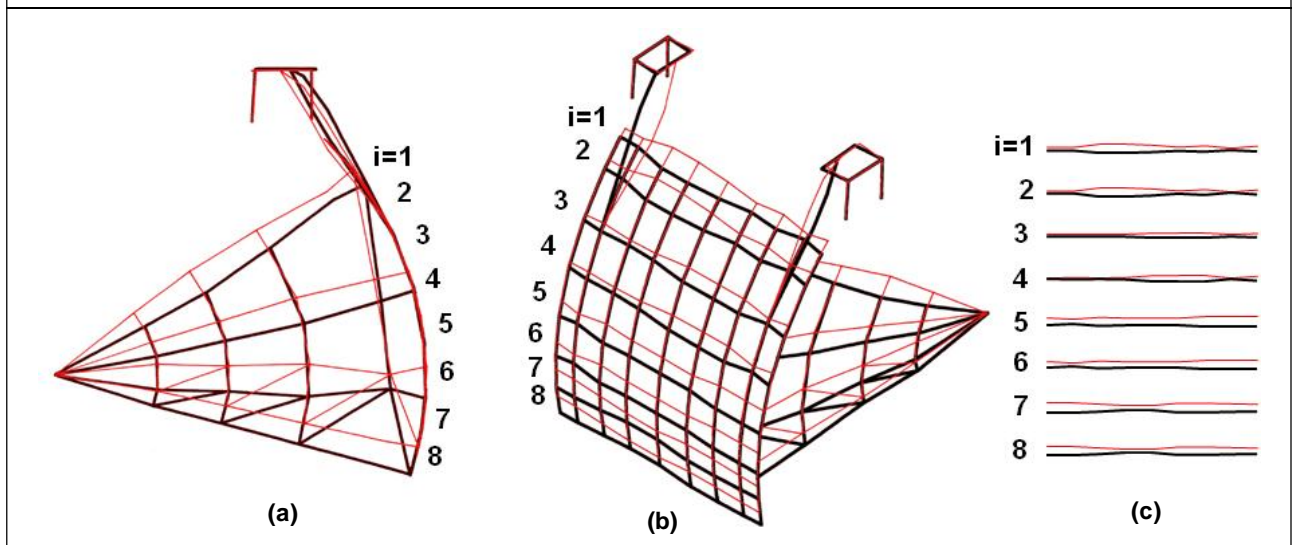
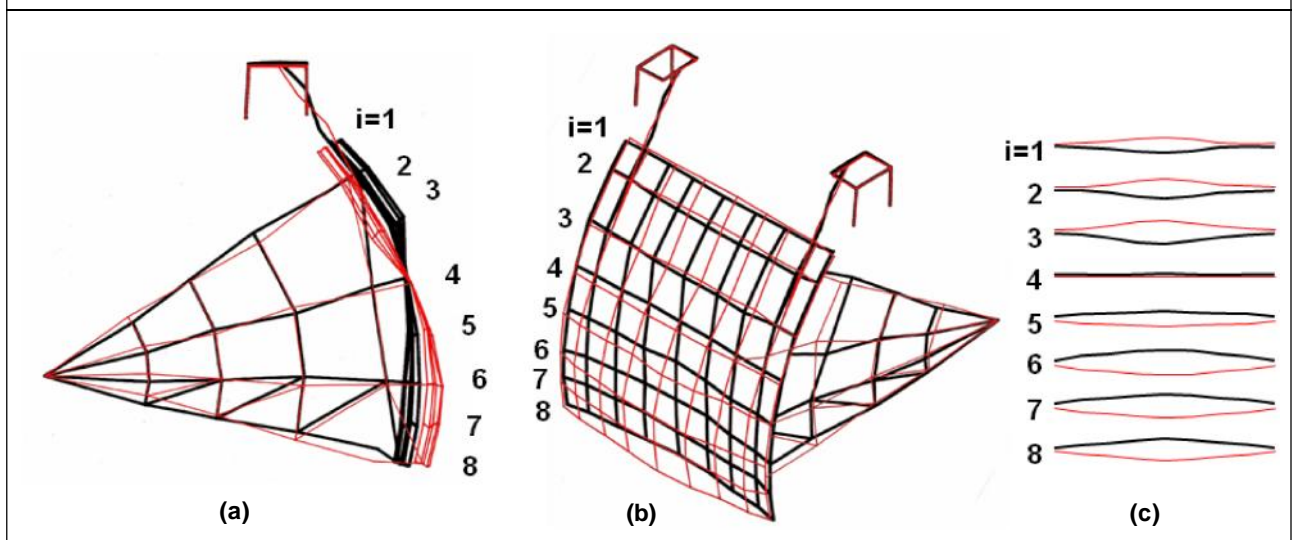


Figure 12: Fundamental Mode Shape of Skinplate Streamwise Bending Vibration for the Original Folsom Dam Tainter Gate Designated as Mode  $M_{x2}$  ( $h_a = 26.9$  Hz;  $\zeta_a = 0.002$ ) Showing (a) The Side View, (b) A 3D-View, and (c) The Spanwise Distributions of Deflection Amplitudes



amplitudes are enlarged to provide easy recognition of the mode shapes.

Figure 11 shows the most significant mode  $M_{z2}$ , which corresponds to rotational vibration of the whole gate around the trunnion pin. The heavy chains and the hoist frames provide

elastic support. The natural vibration frequency of this mode was 6.88 Hz, and the damping ratio was 0.012.

Figure 12 shows the fundamental mode  $M_{x2}$ , which corresponds to the streamwise bending vibration of the skinplate, associated



with the deformation of the radial arm structures. In the vertical direction, the skinplate amplitude corresponds to about a 3/4-wavelength bending mode, as shown in Figure 12a. In the spanwise direction, there is also non-uniformity in the vibration amplitude, approximating a half wavelength mode, with nodes at the spanwise ends, as shown in Figures 12b and 12c. The natural vibration frequency of this mode was 26.9 Hz, and the damping ratio was very small, with a value of 0.002.

After the failure, the remaining Folsom Tainter gates were reinforced. Additional plates were welded onto the radial arms, additional diagonal members were attached between radial arms, additional diagonal braces were attached between cross beams, additional girder bracings were added, and all joints were welded. No changes were made to the skinplate. Additional corresponding experimental modal analyses were made on

a reinforced gate. Results from the modal analyses, given in Figure 13, show the fundamental mode  $N_{x2}$ , involving a streamwise bending vibration of the skinplate. Figure 13a shows a side view and Figure 13b shows the 3D view of the gate. Figure 13c shows the spanwise vibration amplitude distribution at labeled heights. As shown in Figures 13b and 13c, the skinplate vibrated in a bending mode, similar to the mode  $M_{x2}$ . The nodal line is located just a bit higher than that for the original gate, between  $i=3$  and 4 (compare with Mode  $M_{x2}$  in Figure 12). The skinplate still exhibited a half wavelength spanwise mode shape, with nodes at the spanwise ends. The natural vibration frequency of this mode was 27.9 Hz, and the damping ratio was 0.004. Both the natural vibration frequency and damping ratio are slightly larger, relative to the original gate.

Measured natural vibration characteristics of the original and reinforced gates are summarized in Table 3, including sketches of

Figure 13: Fundamental Mode Shape of Skinplate Streamwise Bending Vibration for the Reinforced Folsom Dam Tainter Gate Designated as Mode  $N_{x2}$  ( $f_a = 27.9\text{Hz}$ ;  $\zeta_a = 0.004$ ) Showing (a) The Side View, (b) A 3D-View, and (c) The Spanwise Distributions of Deflection Amplitudes

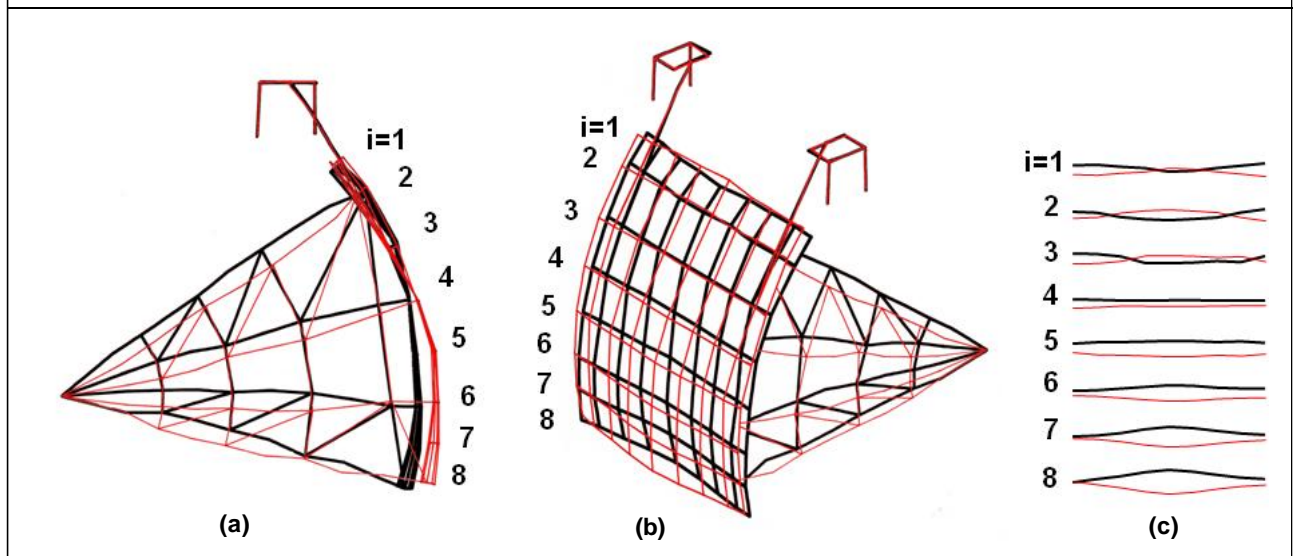
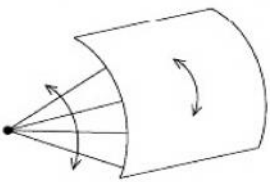
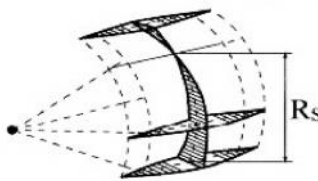


Table 3: Mode Shapes, Modal Frequencies, and Modal Damping from Experimental Modal Analysis of Folsom Dam Tainter Gate In Air

Original Gate				Vibration Mode Shape	Reinforced Gate			
Mode Group	Mode Name	Frequency (Hz)	Damping Ratio		Mode Group	Mode Name	Frequency (Hz)	Damping Ratio
$M_{z2}$	$M_{z21}$	6.88	0.012		$N_{z2}$	$N_{z21}$	6.75	0.009
	$M_{z22}$	7.50	0.021			$N_{z22}$	7.75	0.019
	$M_{z23}$	8.63	0.008			$N_{z23}$	8.00	0.017
$M_{x2}$	$M_{x21}$	26.9	0.002		$N_x$	$N_{x2}$	27.9	0.004
	$M_{x22}$	27.3	0.006			$N_{x3}$	29.0	0.008
	$M_{x23}$	28.8	0.008			—	—	—

the vibration mode-shapes. There are three apparent natural vibration modes of the whole gate in rotation around the trunnion pin, which are grouped into mode group  $M_{z2}$  and  $N_{z2}$  for the original and reinforced gate, respectively.

Since the gate mass was increased by reinforcement, the natural vibration frequencies after reinforced were reduced, except mode  $N_{z2}$  which showed an anomalous slight increase, possibly due to increased stiffness for this mode. In the streamwise direction, there are also three apparent bending modes for the skinplate for the original gate, but only two for the reinforced gate. These streamwise skinplate bending modes are grouped into mode groups  $M_{x2}$  and  $N_x$ , for the original and reinforced gates, respectively. The natural vibration frequencies after reinforcement increased about 1 to 2 Hz. This increase is due to the increased bending rigidity of the skinplate resulting from the reinforcement of the radial arm structures. The damping ratios are quite small, even after reinforcement, with values of 0.008 to 0.021 for the whole gate

rotational vibration around the trunnion pin, and 0.002 to 0.008 for the skinplate streamwise bending vibration.

The spring constant due to the elastic chains and hoist frames and the moment of inertia of the whole gate around the trunnion pin determine the natural vibration frequency of 6.88 Hz, measured for the vibration mode  $M_{z21}$ . As a check, calculations for the spring constant due to the chains and the hoist frames were made to obtain a value of  $1.18 \times 10^8$  N/m. Additionally, calculations for the moment of inertia of the whole gate around the trunnion pin also were made to obtain a value of  $1.309 \times 10^7$  kgm<sup>2</sup>. A natural vibration frequency of 6.85 Hz for the whole gate rotation around the trunnion pin was found, which is quite close to the measured value of 6.88 Hz. One may therefore have confidence that the vibration mode  $M_{z2}$  is indeed that of the whole gate undergoing rigid-body rotational vibration around the trunnion pin, due to the elastic support from the chains and hoist frames.

## Vibration Characteristics from FEM Analysis of the Folsom Dam Tainter Gate

### Vibration Analysis

The natural vibration frequencies and vibration modes were analyzed using FEM analysis software (MSC/N4W, NASTRAN for Windows V3 by the MacNeal-Schwendler Co.). The analyzed frequency range was 0 to 50 Hz, the same range as the experimental modal analysis. The vibration modes obtained by calculation are shown by animation on a computer screen. The natural vibration modes were identified as those modes for which the whole gate was carrying out orderly vibration. The significant results are shown in Figures 14 and 15. Figures 14a and 15a are side views, while Figures 14b and 15b are 3-dimensional downstream views. The red and black lines show the instantaneous vibration shapes with maximum amplitude. In order to help with visualization of the modes, the amplitudes are magnified.

Figure 14 shows the whole gate rotational vibration mode around the trunnion pin with the frequency of 7.3 Hz. This vibration mode is in good agreement with the experimental modal analysis result shown in Figure 11. Deformations are not apparent for any beams of the gate. It appears that this vibration is caused by the elastic support of the chains, which raise and lower the gate.

Figure 15 shows the skinplate streamwise vibration mode. In the streamwise vertical plane, the skinplate is performing the lowest frequency bending mode vibration with the node near the second horizontal girder. In the horizontal plane, the skinplate is performing a half wavelength vibration with nodes near each side of the skinplate. The natural vibration frequency is 25.4 Hz. This vibration mode is in good agreement with the experimental modal analysis result shown in Figure 12.

The vibration frequencies and mode shapes obtained by FEM analysis are listed in Table

Figure 14: Whole Gate Vibration Mode of  $h_a = 7.3$  Hz from FEM Analysis

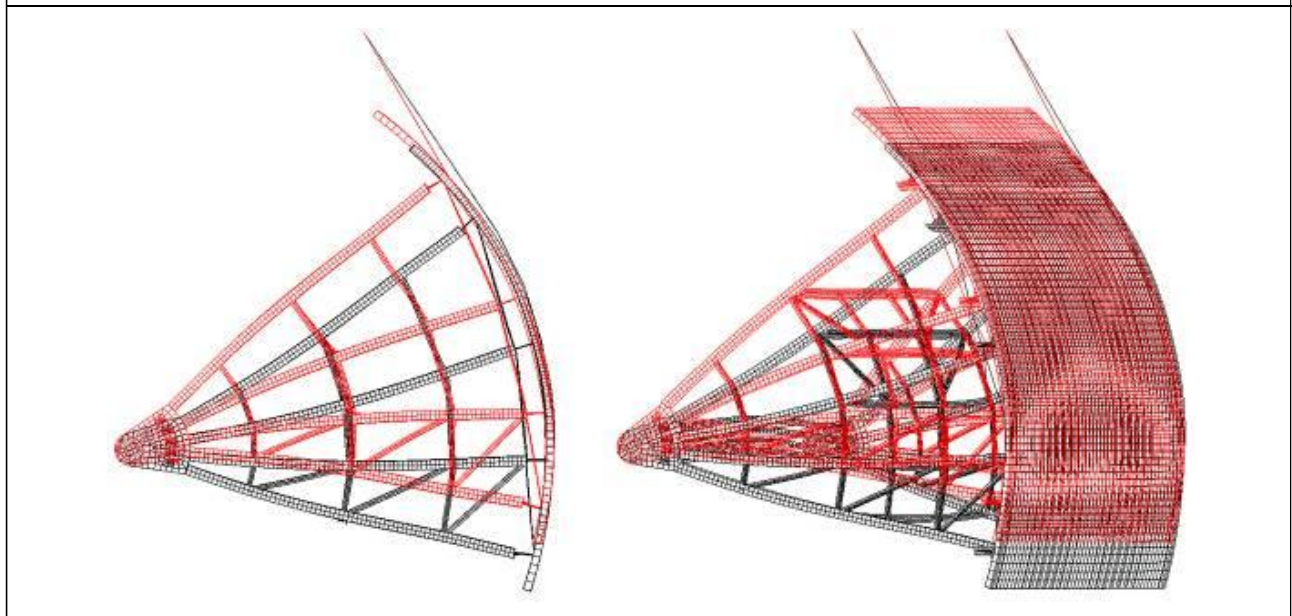


Figure 15: Skinplate Streamwise Vibration Mode of  $h_a1= 25.4$  Hz from FEM Analysis

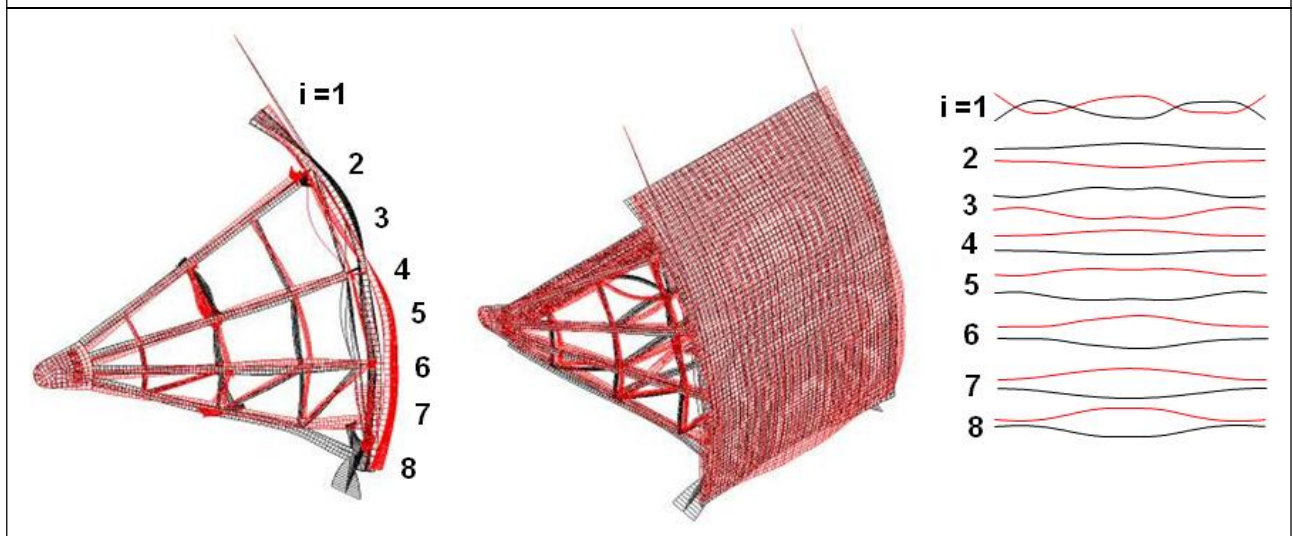


Table 4: Comparison of FEM Analysis Prediction of Modal Frequencies for Fundamental Mode Vibrations of Folsom Dam Tainter Gate with Frequencies from Experimental Modal Analysis

Mode	Vibration Mode shape	Exp. Modal analysis		FEM analysis		Relative Error of Freq. [%]
		Frequency [Hz]	Damping Ratio	Frequency [Hz]	Damping Ratio	
M <sub>z2</sub>		6.88	0.012	7.28	—	5.8
M <sub>x2</sub>		26.9	0.002	25.4	—	5.6

4, where the results from the experimental modal analysis are also shown for comparison. The FEM analysis results for natural vibration frequencies are in good agreement with the experimental modal analysis results. The simulated FEM frequencies have relative error of 5.8% for the whole gate vibration, and 5.6% for the skinplate streamwise vibration.

As a result, one may conclude that the present FEM simulation results showed good correlation for natural vibration frequencies and

corresponding mode shapes with the field test results. Therefore, the finite element model has effectively captured the essential physics even for the large-scaled Folsom Dam Tainter gate.

**Static Deformation Characteristics**  
Structural static deformation of the Tainter gate, induced by the hydrostatic pressure, was calculated for the same FEM model that was validated by comparison with the experimental modal analysis results. It is very useful to know what level of deformation the

massive skinplate experiences due to the hydrostatic pressure.

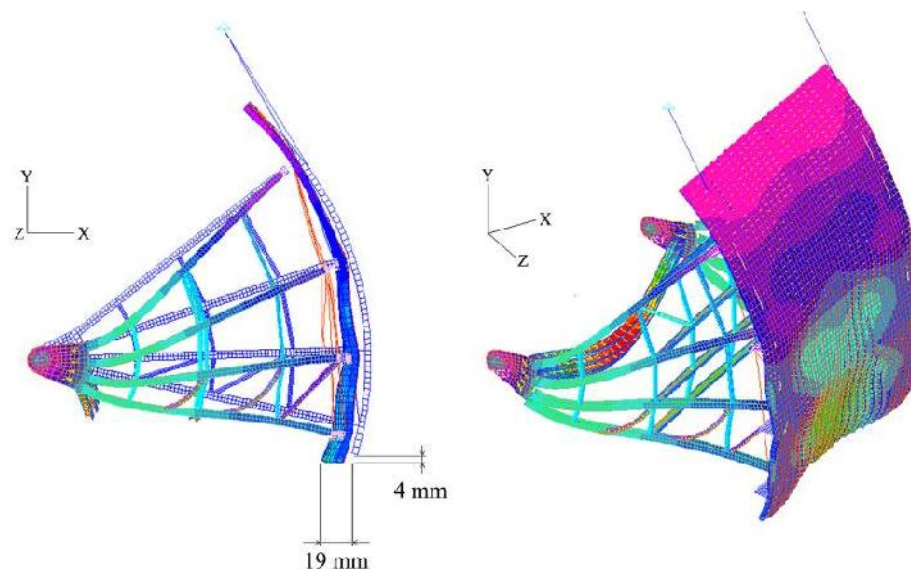
The static deformation was calculated for the gate conditions at the time of failure, that is, at a discharge opening of 0.76 m, and a gate submergence depth was 13.26 m. The whole hydraulic load is  $11.2 \times 10^6$  N. Each elemental hydrostatic load acted on each skinplate element submerged in water, in the direction normal to the skinplate. In addition, the gravity force acted downward on each element of the whole gate.

In Figure 16a, the calculated loading is shown in a side view overlapped with the gate before deformation. Figure 16b is the 3-dimensional view from the upstream side. The skinplate does not show any meaningful deformation in its upper portion, and shows its maximum static deformation at the bottom center portion. Deformation at each side of the skinplate is comparatively small. This limited deflection is because the sides of skinplate

are supported by the radial arms. The trunnion beams show large deformations, but they do not become a problem.

The most significant result is that, as shown in Figure 16a, the bottom center of the skinplate shows a deformation of 19 mm in the downstream direction. The downward deformation of 4 mm is due to the structural deformation of the skinplate itself, in addition to the elastic elongation of the chains. Relatively slender and weak members were used in the Folsom Dam Tainter gate, especially relative to its massive size. These undersized components resulted in the large streamwise deformation of 19 mm. Detailed calculation of the hydrodynamic load due to streamwise vibration (Anami, 2002; Anami *et al.*, 2002, 2005 and 2012) suggest that the hydrodynamic load reaches the same level as hydrostatic load with a vibration amplitude of 8.4 mm along the skinplate spanwise centerline, which is close to half of 19 mm static

Figure 16: Static Structural Deformation of Folsom Dam Tainter Gate with Gate Submergence of 13.26 m at Failure



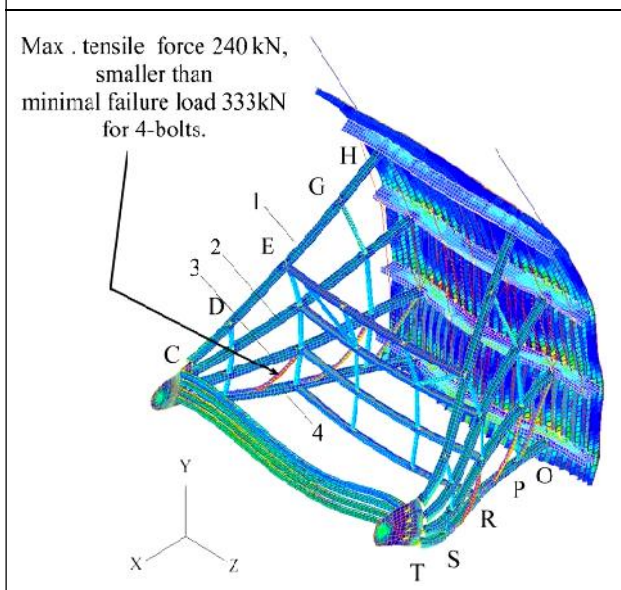
deformation. Therefore, the vibratory deformation of the skinplate cannot be disregarded.

#### Static Tensile Loads and Influence of Frictional Forces

The USBR concluded that the increased trunnion friction was the main factor in gate failure, that is, an excessive static load arose since the gate was raised against the trunnion friction, thus inducing the incipient gate failure. In the USBR analysis of the failure, an FEM analysis was carried out for the given hydrostatic load and trunnion friction to calculate the static stress. Their results suggest that excessive tensile force developed on the diagonal member between 3<sup>rd</sup> and 4<sup>th</sup> arms, exceeding the allowable load of the bolts. Since some doubt remains concerning the validity of FEM model by USBR, it was deemed prudent to re-examine the USBR conclusions by using our previously validated FEM model.

As a result of these considerations, the tensile forces acting on each member in Folsom gate exposed to the loading conditions at the time of failure were analyzed for a gate discharge opening of 0.76 m and a gate submergence depth of 13.26 m, where the trunnion friction coefficient was varied over a range of values, including the USBR-estimated maximum possible value of 0.3 at the moment of gate failure. One of the calculated results, the stress using a trunnion friction coefficient of 0.3, is shown in Figure 17. The significant aspect of this figure is that the maximum stress appears in the diagonal member 3E-4D, that is, the member between 3<sup>rd</sup> and 4<sup>th</sup> arm, as indicated by the orange color. From this load, one can determine that the tensile force acting on the bolted joint of

Figure 17: Static Stress and Tensile Force on Folsom Dam Tainter Gate with Gate Submergence of 13.26 m and Trunnion Frictional Coefficient of 0.3 at Failure

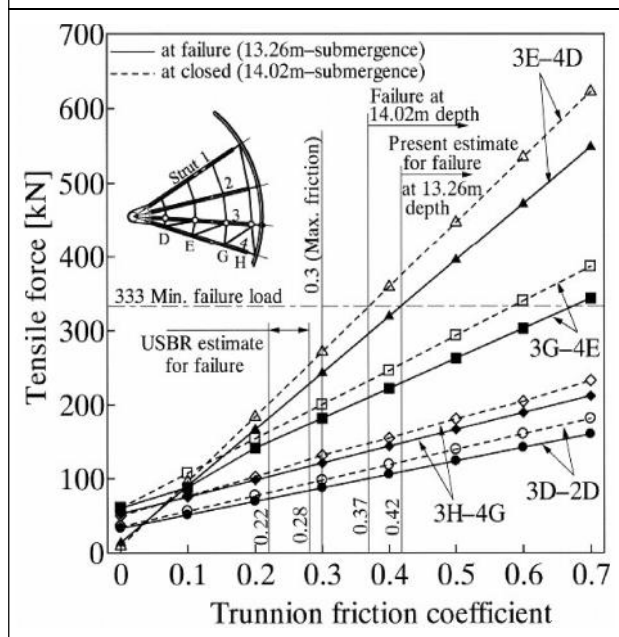


the diagonal member 3E-4D reached a maximum value of 240 kN.

The USBR Forensic Team concluded that the Folsom gate failure started from the breaking of 4 bolts connecting the diagonal member 3E-4D to the 3<sup>rd</sup> and 4<sup>th</sup> radial arms. The Forensic Team recovered similar 4-bolted members and attachment plate and undertook a careful tensile-loading test. As a result, it was confirmed that the range of the tensile failure load was 333 kN to 363 kN. The calculated maximum tensile force of 240 kN from the present FEM analysis, which is still sufficiently less than the failure load of 333 kN, leads to the conclusion that the static load alone did not produce the observed failure.

The maximum tensile force on the diagonal members between arms was carefully calculated with an increasing trunnion friction coefficient up to 0.7, as shown by the solid line in Figure 18. As shown by the solid symbols,

Figure 18: Tensile Loads on Strut Brace with Increasing Trunnion Friction Coefficient Up to 0.7



the calculated data increased linearly with increasing trunnion friction coefficient, and hence the data are connected with the solid lines. If the trunnion friction coefficient is smaller than about 0.1, the maximum tensile force appears in the center diagonal member 3G-4E, while if it exceeds about 0.1, the maximum tensile force appears in the diagonal member 3E-4D near the trunnion pin. The maximum tensile force in member 3E-4D exceeds the failure load of 333 kN, only when the trunnion friction coefficient reaches 0.42. This value is far larger than the range of 0.22 to 0.28, which was estimated by USBR to be reasonable values for failure. In addition, this value of 0.42 is still larger than the maximum possible friction coefficient 0.3, which was obtained by USBR from friction tests on the trunnion pin of the failed gate.

The validated FEM model results indicate that it was not possible for the Folsom Tainter

gate to fail only due to the excessive static load resulting from the increased trunnion friction, as the Forensic Team concluded.

Supposing nonetheless that the trunnion friction was the main cause of the Folsom gate failure, logic then dictates that failure should have occurred immediately upon opening the gate, that is, when the gate submergence depth was near its maximum value and larger than 13.26 m recorded at the time of the failure. The gate submergence depth for the closed gate was 14.02 m, since the Folsom gate failed at the gate submergence depth of 13.26 m and the discharge opening of 0.76 m. Therefore, upon incipient gate opening, the gate submergence depth was about 6% larger than that at the moment of failure, thus resulting in a correspondingly larger hydrostatic pressure load and in a correspondingly larger influence of trunnion friction. Supposing the trunnion friction to be the cause of gate failure, one must then accept that the accident should have occurred at the beginning of the gate opening process.

Based on this reasoning, FEM calculations were made again at the condition (the gate submergence depth of 14.02 m) when the gate started to open, to re-examine the maximum tensile forces on the diagonal members. The calculated results for the gate closed are shown by the open symbols and broken lines in Figure 17. The tensile forces are about 12% larger than those at the gate opening of 0.76 m where failure occurred. However, the tensile force for values of trunnion friction coefficient in the range of 0.22 to 0.28 is still significantly smaller than the minimum failure load of 333 kN. Moreover, not until a frictional coefficient value of 0.37 (which is still larger than the

maximum frictional coefficient of 0.3 estimated at the time of gate failure) does the maximum tensile force exceed the failure load of 333 kN.

The above results, in summary, suggest that increased trunnion friction alone could not have been the only contributing mechanism of the Folsom gate failure.

### Predicted Closed Energy Cycle

As a result of the field vibration tests and the FEM analysis, the gate has been shown to possess two typical and relevant natural vibration modes, as illustrated in Figure 19. One fundamental vibration mode is the rigid-body rotational lifting vibration of the whole gate about the trunnion pin, denoted by  $\Theta$ . The second significant mode of vibration was lowest frequency streamwise bending of the skinplate (see the dotted lines), denoted by  $\Psi$ . This lowest frequency bending mode of the skinplate is essentially a streamwise rotation of the skinplate about a point in the upper half of the skinplate. When the massive skinplate,

which constitutes 68% of the whole gate mass, performs a rotational vibration, a large inertia torque due to this rotational vibration arises, which can then excite the whole gate to vibrate around the trunnion pin. When the whole gate vibrates around the trunnion pin, an additional inertia torque also arises, which can produce additional skinplate rotation. If the natural frequencies of these two vibration modes coincide, the streamwise rotational vibration of the skinplate and the whole gate rotational vibration around the trunnion pin can couple with each other through the inertia torques, resulting in "coupled-mode vibration".

Such a coupled-mode vibration will be accompanied by a flow-rate variation beneath the gate. The flow-rate variation produces pressure fluctuations, which, under certain conditions, can lead to a violent self-excited vibration, which is then called "coupled-mode self-excited vibration". The closed-loop energy cycle for coupled-mode self-excited vibration is shown in Figure 20. Also shown in Figure 20 is the "push-and-draw hydrodynamic pressure," which is a significant factor in gate failure. Details of this closed energy loop are discussed in the following paragraphs.

If the streamwise vibration of the skinplate is triggered by some random excitation, the skinplate inertia torque excites the whole gate to vibrate around the trunnion pin. The streamwise skinplate vibration and the whole gate rotation produce a change in the gate opening, resulting in a flow-rate variation beneath the gate, inducing a "flow-rate variation pressure". If the lower end of the skinplate behaves as a press-shut device (see Naudascher and Rockwell, 1993 for a discussion of press-open and press-shut

Figure 19: Two Predominant Natural Vibration Modes of Folsom Dam Tainter Gate

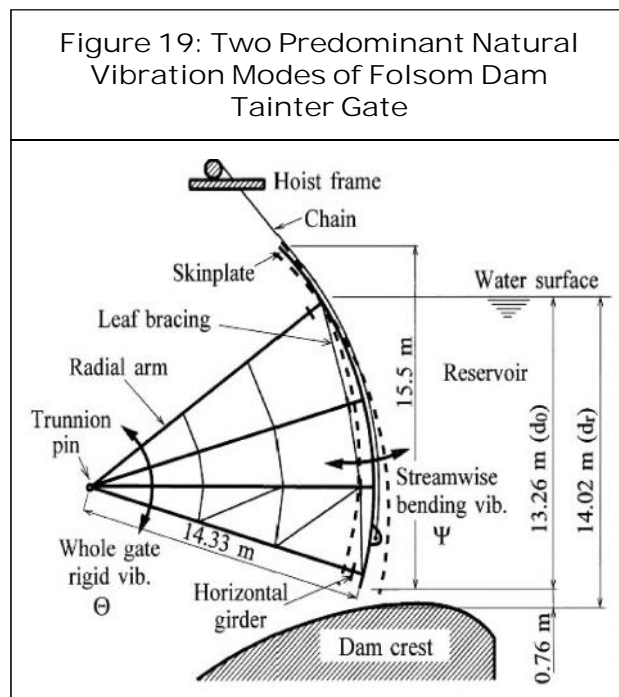
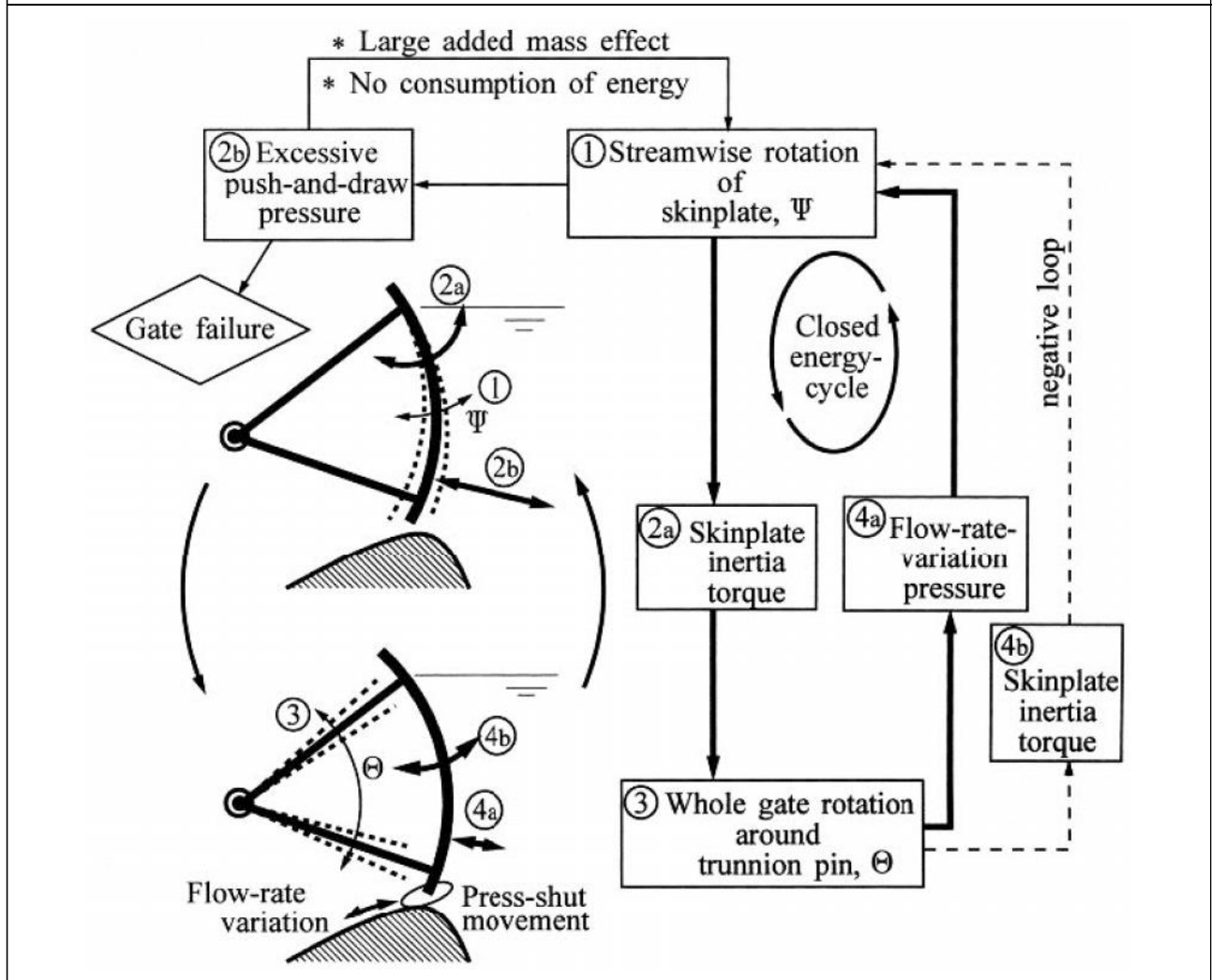




Figure 20: Closed Energy Cycle for Coupled-Mode Flow-Induced Vibration, Possible Tainter Gate Susceptibility



devices), the flow-rate-variation pressure feeds energy back to the skinplate streamwise vibration, thus amplifying its vibration amplitude, as shown near the bottom of Figure 20. As a result, when the lower end of the skinplate exhibits press-shut behavior, violent coupled-mode self-excited vibration may occur.

The coupled inertia torque acting on the skinplate due to the whole gate vibration around the trunnion pin actually serves to stabilize the gate due to its phasing relative to

the skinplate motion. The negative excitation of this inertia torque is shown by the dashed line in Figure 20. However, the stabilizing effect of the inertia torque from the whole gate vibration is comparatively small. It is significant to note that this type of coupled-mode self-excited vibration can occur, even when the skinplate center is concentric with the trunnion pin.

Of special note in this closed energy-cycle is that the streamwise skinplate vibration induces a push-and-draw pressure. The

amplitude of this push-and-draw pressure can be more than 10 times that of the flow-rate variation pressure, and it could have potentially caused the Folsom Dam gate failure. The gate fails when the loading due to the push-and-draw pressure exceeds the material strength.

It is also significant that the push-and-draw pressure does not consume energy from the vibrating gate. The push-and-draw pressure has associated with it a large added mass effect. This large added mass of water must be accelerated with the gate as it undergoes its streamwise vibration. The added mass lowers the relatively high in-air frequency of the streamwise skinplate vibration. As a result, when the in-water streamwise skinplate vibration frequency approaches the frequency of the in-water whole gate rigid body rotational vibration, the system approaches resonance. Near resonance, the comparatively small amplitude flow-rate variation pressure can spontaneously amplify the amplitude of coupled-mode vibration.

#### Model Investigations of Coupled-Mode Self-Excited Vibration

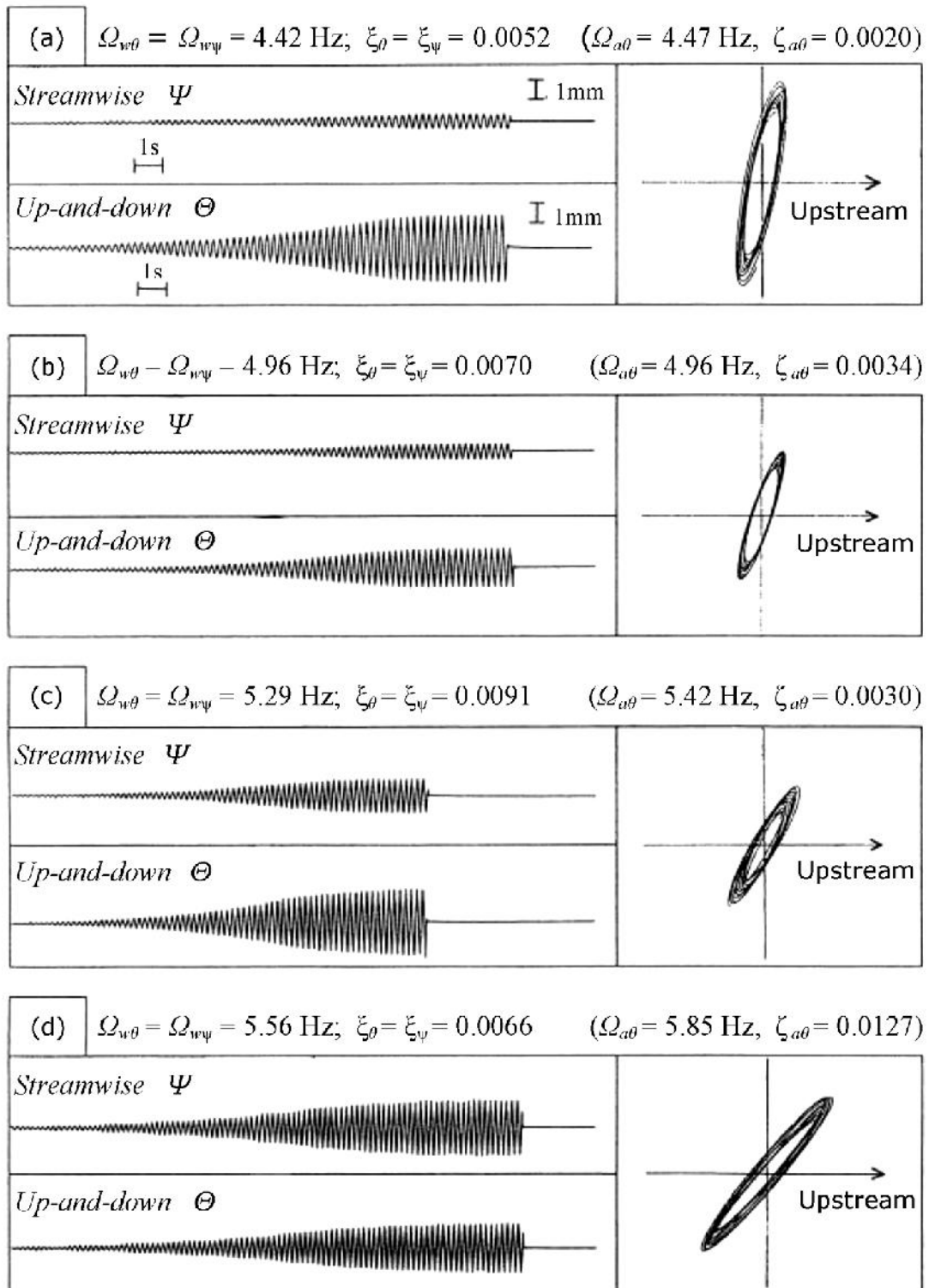
The model gate was constructed to confirm the coupled-mode self-excited vibration mechanism just postulated in the preceding section. In addition, the data obtained concerning the coupled-mode vibration of the streamwise skinplate bending rotation and the whole gate rotation will be used subsequently to verify the theoretical analysis of this mechanism.

Figure 21 shows typical records of the self-excited vibration waveforms at  $F_0 = 16.0$ , which were measured at the lower end of the

gate. The upper waveforms show the streamwise vibration  $\Psi$ , and the lower show the up-and-down vibration  $\Theta$ . It was previously accepted that a gate with the skinplate concentric with the trunnion center could never undergo any self-excited vibrations. However, the model gate clearly undergoes spontaneous vibrations, exponentially increasing in amplitude, and approaching a steady vibration with a constant amplitude. These test results clearly demonstrate that Tainter gates essentially possess an inherent dynamic instability, even if the skinplate is non-eccentric to the trunnion pin.

Diagrams on the right side in Figure 21 show the vibration trajectories of the lower end of the skinplate. In all cases, the vibration trajectory exhibits the characteristic counterclockwise behavior of a press-shut device. The gate opening is reduced when the skinplate moves in the downstream direction. In the case of Figure 21a, where the in-air whole gate vibration takes the frequency  $\Omega_{a_r}$  of 4.42 Hz and the damping ratio  $\zeta_{a_r}$  of 0.0020, the trajectory has a steep slope. Both the excitation ratios,  $\zeta_{a_r}$  and  $\zeta_{\Theta}$ , measured from the exponentially increasing vibration-waveforms, were 0.0052. As  $\Omega_{a_r}$  increases to 4.96 Hz as in Figure 21b and to 5.29 Hz as in Figure 21c, the streamwise vibration increases in amplitude, and as a result, the trajectory inclination becomes smaller. Accordingly, the excitation ratio also increases to 0.007 in Figure 21b and to 0.0091 in Figure 21c. Furthermore, when  $\Omega_{a_r}$  is 5.85 Hz, as in Figure 21d, the up-and-down and streamwise vibrations have nearly equal amplitudes, resulting in a trajectory inclination of  $45^\circ$ . In this configuration, the gate motion can most

Figure 21: Self-Excited Vibration Waveforms and Trajectories for 1/31-Scaled Model of the Folsom Dam Gate at  $F_0 = 16.0$  ( $d_0 = 420$  mm,  $h_{ae} = 12.3$  Hz) for Four Different In-Air Whole Gate Vibration Frequencies



effectively extract energy from the fluctuating flow, resulting in a relatively large excitation ratio of 0.0066 in spite of the fairly large in-air damping ratio of 0.0127.

Measured data for in-water vibration frequency are plotted in Figure 22a, where data from two test results for the basic Froude number  $F_0 = 13.9$  and  $16.0$  are shown. The abscissa is the frequency ratio  $\chi_{nw} (= \Omega_{nw} / \Omega_{a_e})$  of the streamwise in-water natural vibration frequency  $\Omega_{nw}$  to the in-air natural vibration frequency around the trunnion,  $\Omega_{a_e}$ , where  $\Omega_{a_e}$  was varied from 2.6 Hz to 7.3 Hz, and  $\Omega_{nw}$  took a constant value of 6.14 Hz for  $\Omega_{a_e} = 10.6$  Hz and 6.10 Hz for  $\Omega_{a_e} = 12.3$  Hz, respectively. When the frequency ratio  $\chi_{nw}$  is larger than 1.0, the in-water to in-air frequency ratio,  $\chi_{w_e} (= \Omega_{w_e} / \Omega_{a_e})$ , of the whole gate vibration around the trunnion becomes 1.0, and the frequency ratio  $\chi_{w_e} (= \Omega_{w_e} / \Omega_{a_e})$  of the streamwise in-water vibration to the in-air vibration around the trunnion also becomes 1.0. Thus, one may conclude that the vibration is synchronized with the whole gate natural vibration (the lower of the two frequencies). In contrast, when  $\chi_{nw}$  is slightly less than 1.0, both frequency ratios,  $\chi_{w_e}$  and  $\chi_{w_{e_e}}$ , take on the same value as the abscissa,  $\chi_{nw}$ . Thus, one may conclude that the vibration is synchronized with the skinplate streamwise natural vibration (again, the lower of the two frequencies). When  $\chi_{nw}$  becomes still smaller, the vibrations do not synchronize.

The dynamic similarity of the fluctuating flow due to skinplate streamwise vibration is subject to the Froude number  $F$ , (different from the basic Froude number  $F_0$ ) defined by

$$F \equiv 2f \sqrt{\frac{d_0}{g}} \Omega_{w_e} \quad \dots(3)$$

In the present model tests, the Froude number  $F$  ranged from 3.4 to 7.9 for  $F_0 = 13.9$  and from 3.5 to 7.7 for  $F_0 = 16.0$ .

The exponentially increasing or decreasing vibration waveforms suggest a significant characteristic of the self-excitation due to fluid motion called the “fluid-excitation ratio”. If the in-air damping ratios  $\delta_{a_e}$  and  $\delta_{a_{eE}}$ , due to mechanical and additional damping, were measured, one may calculate from any spontaneous vibration waveforms, the fluid-excitation ratio for the whole gate vibration,  $\zeta_{f_e}$ , and that for the streamwise vibration,  $\zeta_{f_e}$ , by the following expressions, respectively:

$$\zeta_{f_e} \left( \equiv \frac{\Delta C_{c_e}}{2I_e \Omega_{a_e}} \right) = \frac{\zeta_{e_e}}{\chi_{w_e}} + \delta_{a_e} \quad \dots(4a)$$

$$\zeta_{f_{eE}} \left( \equiv \frac{\Delta C_{c_{eE}}}{2I_{eE} \Omega_{a_{eE}}} \right) = \frac{\zeta_{e_{eE}}}{\chi_{w_{e_{eE}}}} + \delta_{a_{eE}} \quad \dots(4b)$$

where  $\zeta_{e_e}$  and  $\zeta_{e_{eE}}$  are the resultant excitation ratios for the streamwise and whole gate vibrations.

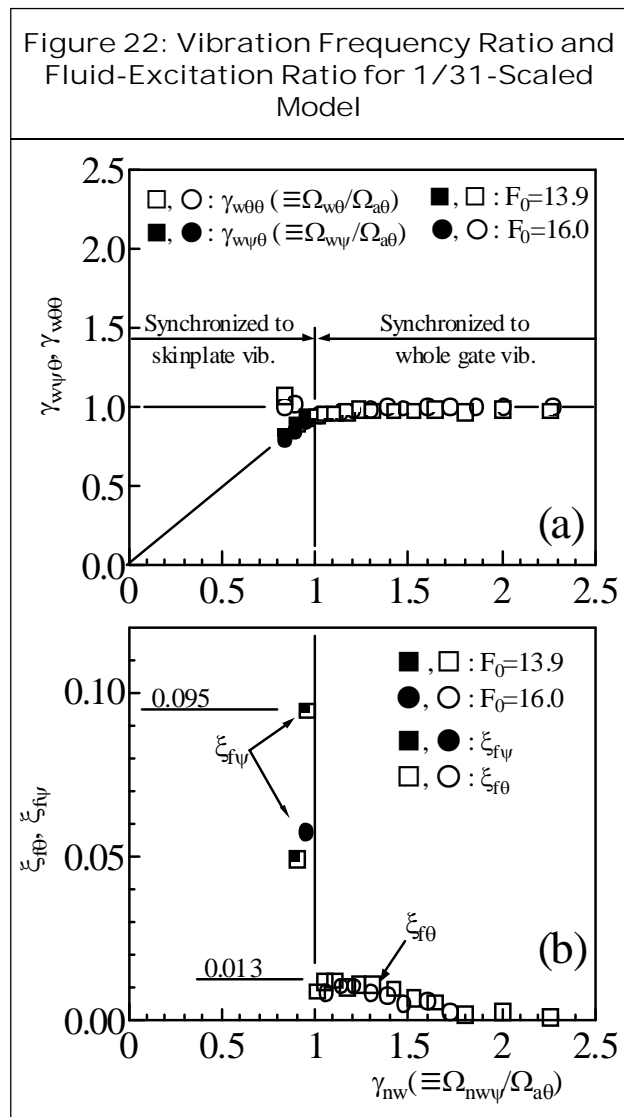
In the present model gate, the mean value of  $\delta_{a_e}$  was 0.003 from in-air free vibration tests of the whole gate around the trunnion. In the case of model experiments, a fairly large damping effect appears for the skinplate streamwise vibration, due to leakage flows from comparatively large clearances kept at both sides of the skinplate. This kind of additional damping is intrinsic to a model experiment and cannot be avoided. For a measure of the effect of these leakage flows, in-water free vibration tests of the skinplate were made in detail to measure the damping ratio including this additional damping effect. As a result, the damping ratio of the skinplate streamwise vibration,  $\delta_{a_{eE}}$  was 0.13 for  $F_0 = 16.0$  and 0.11 for  $F_0 = 13.9$ .

Calculated values of the fluid-excitation ratios based on experimental data are plotted in Figure 22b. Over the frequency range of  $\chi_{nw}$ , larger than 1.0, an instability that is synchronized with the whole gate vibration appears, and the maximum value of the fluid-excitation ratio  $\xi_{f_r}$  is 0.013. If  $\chi_{nw}$  becomes slightly smaller than 1.0, the instability is synchronized with the skinplate vibration, and the fluid-excitation ratio  $\xi_{f_r}$  rapidly increases, showing a maximum value of 0.095 and then rapidly decreases with a further decrease in  $\chi_{nw}$ .

### CONCLUSION

Based on eyewitness accounts and on a validated FEM analysis, it would appear very likely that flow-induced vibrations must have played a role in the failure of the Folsom Dam Tainter gate in 1995. At the time when the USBR Forensics Team completed its report, the mechanism of coupled-mode self-excited vibration of Tainter gates had not been formulated. Other than the “eccentricity-instability” that had been developed as a result of the Wachi Dam gate failure, there was no known mechanism for the vibration of such a massive Tainter gate. With no significant eccentricity between the skinplate center and the trunnion center, the Forensics Team ruled out the possibility of the “eccentricity instability,” and chose not to consider any other vibration-inducing mechanism. They ignored the testimony of the operator who was on the catwalk above the gate at the time of its failure, when based on an unvalidated FEM model, they concluded that the gate failed due to static loading resulting from corrosion and increase trunnion pin friction. The fallacy in this conclusion, in addition to ignoring first hand observation, is that the failure should have occurred immediately upon opening the gate, not after having opened the gate 0.76 m.

The present study provides measured mode shapes, frequencies and damping ratios for an original Folsom Dam gate, similar to the failed gate, and for the a Folsom Dam gate after a retrofitted reinforcement. A high precision FEM model of the original Folsom Dam gate yielded frequencies and mode shapes consistent with the measured dynamics of the original gate. This same FEM model showed that the loading on the diagonal



member 3E-4D near the trunnion pin, identified as the point of failure by the USBR, did not exceed the minimum failure load as measured by the USBR. Even upon incipient gate opening, the loading, which was more than 12% higher than with the gate open at 0.76 m, did not exceed the minimum loading for failure. There is strong evidence that the gate did not fail due to static loading as was concluded by the USBR Forensics Team.

On the basis of the eyewitness testimony and through a persistent fifteen-year research program the mechanism of the coupled-mode self-excited dynamic instability of Tainter gates has been formulated. The mechanism involves the coupling of two modes, in this case the rigid-body rotation about the trunnion pin and a low frequency bending mode of the skinplate. When the two modal frequencies coalesce due to the added mass effect of the water environment, the inertial and hydrodynamic loadings create a situation whereby the motion of one mode serves as the forcing function for the other mode. A 1/31 scaled model of the Folsom Dam gate was used to verify the existence of this instability mechanism. Further testing has been undertaken and a theoretical model of the mechanism has been developed. Future papers by the present authors will report on these studies.

It is hoped that through this presentation of the data in this paper, an awareness of the coupled-mode self-excited instability mechanism may be fostered among gate designers and in the general gate engineering community. The coupled-mode self-excited instability mechanism can lie dormant until some hard input causes an initiation of the vibration, which then quickly leads to gate

failure. An understanding of the mechanism is the first step in designing gates that are not susceptible to this instability mechanism.

Retrospectively, after identification of the coupled-mode self-excited dynamic instability, reexamination of the Wachi gate failure showed that the coupled-mode self-excitation mechanism is consistent with the gate vibration in the Wachi failure. The unknown mechanism of gate vibration that was suspected at the time of the Wachi failure (Ishii *et al.*, 2008) has now been plausibly identified. In the authors' opinion, this dynamic instability mechanism also played a major role in the Folsom Dam gate failure. The information contained in this paper has been previously presented to the USBR. The existence of this coupled-mode dynamic instability is significant and must be understood by gate designers, owners, and operators to avoid future gate failures. In an effort to educate the gate engineering community, the research leading to the identification of this instability mechanism is documented in this paper. The authors' hope is that others can understand this mechanism and the role it most likely played in the Folsom Dam gate failure.

## ACKNOWLEDGMENT

Financial support was provided by the Bureau of Reclamation, US Department of the Interior, and through a Science and Research Grant from the Japanese Ministry of Education. The authors would like to express their sincere and great thanks to Mr. Tom Aiken, Mr. Charles Howard, Mr. Steve Herbst, Mr. John White, Mr. Steve Sherer and Mr. Bill Joy, for their kind support in undertaking this study of the Folsom Dam gate failure. The authors would like to express their sincere thanks to Mr. Keiji

Sakamoto and Mr. Shigeharu Mima, for their kind support in conducting the impact hammer field tests and also performing computer calculations for the modal analysis. 🌐

## REFERENCES

1. Anami K (2002), "Flow-Induced Coupled-Mode Self-Excited Vibration of Large-Scaled Tainter Gates", Dissertation Submitted to Osaka Electro-Communication University, (in Japanese: Translated into English on Dec. 2005), available from author.
2. Anami K and Ishii N (1998), "In-Air and In-Water Natural Vibrations of Folsom Dam Radial Gate in California", 11<sup>th</sup> International Conference on Experimental Mechanics, pp. 29-34.
3. Anami K, Ishii N and Knisely C W (2012), "Pressure Induced by Vertical Planar and Inclined Curved Weir Plates Undergoing Streamwise Rotational Vibration", *J. Fluids and Structures*, Vol. 29, pp. 35-49.
4. Anami K, Ishii N and Yamasaki M (2000), "Hydrodynamic Pressure Induced by Rotating Skinplate of Folsom Dam Tainter Gate", *Trans. Japan Soc. Mechanical Engineers, Series B*, Vol. 66, No. 652, pp. 3116-3123 (in Japanese).
5. Anami K, Ishii N and Knisely C W (2014), "Theory of Coupled-Mode Self-Excited Vibration of Tainter Gates", Accepted by *Int. J. Mechanical Engineering and Robotics Research*, October.
6. Anami K, Ishii N, Knisely C W and Oku T (2005), "Hydrodynamic Pressure Load on Folsom Dam Tainter Gate at Onset of Failure Due to Flow-Induced Vibrations", Symposium on Flow-Induced Vibration, Proc. of ASME Pressure Vessels and Piping Conference, Vol. 4, pp. 557-564.
7. Anami K, Ishii N, Knisely C W, Todd R V and Oku T (2006), "Vibration Tests with a 1/13-Scaled 3-D Model of the Folsom Dam Tainter Gate and Its Prediction by Theory", Proc. of ASME Pressure Vessels and Piping Conference, Vancouver, PVP2006-ICPVT-11-93917.
8. Imaichi K and Ishii N (1977), "Instability of an Idealized Tainter Gate System Without Damping Caused by Surface Waves on the Backwater of Dam", *Bulletin of the Japan Society of Mechanical Engineers*, Vol. 20, No. 146, pp. 963-970.
9. Ishii N (1995a), "Folsom Dam Gate Failure Evaluation and Suggestions", Report Submitted to US Bureau of Reclamation, August 24.
10. Ishii N (1995b), "Folsom Dam Gate Failure Evaluation Based on Modal Analysis and Suggestion", Report Submitted to US Bureau of Reclamation, November 8.
11. Ishii N (1997), "Dynamic Stability Evaluation for Folsom Dam Radial Gate and Its Inherent Non-Eccentricity Instability", Report Submitted to US Bureau of Reclamation, July 17.
12. Ishii N and Imaichi K (1976), "Instability of an Idealized Tainter Gate System Without Damping Caused by Surface Waves on the Backwater of Dam", *Trans. Japan Soc. of Mechanical Engineers*, Vol. 42, No. 364, pp. 3853-3861 (in Japanese).
13. Ishii N and Imaichi K (1977a), "Water Waves and Structural Loads Caused by

- a Periodic Change of Discharge from a Sluice Gates”, *Bulletin of the Japan Society of Mechanical Engineers*, Vol. 20, No. 6, pp. 998-1007.
14. Ishii N and Imaichi K (1977b), “Instability of Elastically Suspended Tainter Gate System Caused by Surface Waves on the Upstream Channel of a Dam”, *ASME J. of Fluids Engineering*, Vol. 99, No. 4, pp. 699-708.
  15. Ishii N and Imaichi K (1980), “Dynamic Instability of Tainter Gates”, *In Practical Experiences with Flow-Induced Vibrations*, E Naudascher and D O Rockwell (Eds.), Springer, pp. 452-460.
  16. Ishii N and Naudascher E (1984), “Field Tests on Natural Vibration Modes of a Tainter Gate”, *In Channels & Channel Control Structures*, K V H Smith (Ed.), Springer, pp. 209-222.
  17. Ishii N and Naudascher E (1992), “A Design Criterion for Dynamic Stability of Tainter Gates”, *J. Fluids and Structures*, Vol. 6, pp. 67-84.
  18. Ishii N, Anami K, Oku T, Makihata T and Knisely C W (2008), “Analogous Tainter Gate Failures in Japan and USA”, Proc. of the 9<sup>th</sup> International Conference on Flow-Induced Vibration, in Flow Induced Vibration, Zolotarev I and Horacek J (Eds.), pp. 569-574.
  19. KXTV-10 (1995), TV News Broadcast, “The Folsom Dam Gate Failure”, 10 a.m. News, July 17, Sacramento, California.
  20. Naudascher E and Rockwell D (1993), “Flow-Induced Vibrations: An Engineering Guide”, IAHR/AIRH Hydraulic Structures Design Manual 7 Hydraulic Design Considerations, Amsterdam, Balkema.
  21. Yano K (1968), “Wachi Dam Tainter Gate Failure”, Annual Report of Disaster Prevention Research Institute Kyoto University, No. 11, B, pp. 203-219 (in Japanese).
-